

1947

Radio-frequency radiation from electric discharges in gases

Willis Laurens Emery
Iowa State College

Follow this and additional works at: <https://lib.dr.iastate.edu/rtd>



Part of the [Electrical and Electronics Commons](#)

Recommended Citation

Emery, Willis Laurens, "Radio-frequency radiation from electric discharges in gases " (1947). *Retrospective Theses and Dissertations*. 12417.
<https://lib.dr.iastate.edu/rtd/12417>

This Dissertation is brought to you for free and open access by the Iowa State University Capstones, Theses and Dissertations at Iowa State University Digital Repository. It has been accepted for inclusion in Retrospective Theses and Dissertations by an authorized administrator of Iowa State University Digital Repository. For more information, please contact digirep@iastate.edu.

NOTE TO USERS

This reproduction is the best copy available.

UMI[®]

**RADIO-FREQUENCY RADIATION FROM
ELECTRIC DISCHARGES IN GASES**

by

Willis Laurens Emery

**A Thesis Submitted to the Graduate Faculty
for the Degree of**

DOCTOR OF PHILOSOPHY

Major Subject: Electrical Engineering

Approved:

Signature was redacted for privacy.

In Charge of Major Work

Signature was redacted for privacy.

Head of Major Department

Signature was redacted for privacy.

Dean of Graduate College

Iowa State College

1947

UMI Number: DP11816

INFORMATION TO USERS

The quality of this reproduction is dependent upon the quality of the copy submitted. Broken or indistinct print, colored or poor quality illustrations and photographs, print bleed-through, substandard margins, and improper alignment can adversely affect reproduction.

In the unlikely event that the author did not send a complete manuscript and there are missing pages, these will be noted. Also, if unauthorized copyright material had to be removed, a note will indicate the deletion.

UMI[®]

UMI Microform DP11816

Copyright 2005 by ProQuest Information and Learning Company.

All rights reserved. This microform edition is protected against unauthorized copying under Title 17, United States Code.

ProQuest Information and Learning Company
300 North Zeeb Road
P.O. Box 1346
Ann Arbor, MI 48106-1346

TABLE OF CONTENTS

	Page
I. INTRODUCTION	1
A. General	1
B. Plasma Oscillations	2
C. Oscillations in a Potential	
Minimum	7
D. Periodic Interruption of the	
Current	9
E. The Problem	13
II. EXPERIMENTAL APPARATUS	18
A. General	15
B. Preparation of Gases.	18
C. Discharge Tube	22
D. Measurement of Pressure	24
E. Pick-up Probe and Receiver	35
F. Recording Mechanism and	
Auxiliaries	45
III. RESULTS	54
A. Hydrogen	54
B. Oxygen	60

T8306

	Page
IV. DISCUSSION	76
V. SUMMARY	80
VI. REFERENCES	82
VII. ACKNOWLEDGMENT	86
VIII. VITA	87

I. INTRODUCTION

A. General

Considerable work has been done in recent years on radio-frequency oscillations arising from electric discharges in gas. In general this work has proceeded in two distinct areas. One was concerned with the elimination of radio interference arising from coronas in high-voltage installations, precipitation static, arc discharge in gas tubes, and such related phenomena. The emphasis in this work was on the practical means by which such interference might be eliminated or minimized. Only rarely were attempts made to account for the fundamental physical basis for the oscillations. Consequently, none of the papers belonging to this category have been cited here.

The other area of investigation has been more concerned with the fundamental physical phenomenon and only occasionally has considered practical aspects. These papers provided the basis for the present work. Analyses of oscillations in mercury vapor, inert gases and air have been reported.

Three fundamental kinds of oscillations have been recognized and described. The first type are plasma

oscillations which occur in the space where there is a concentration of both positive and negative charges. The displacement of some of these charges disturbs the equilibrium and gives rise to an additional electric field which tends to restore that equilibrium. The presence of this restoring field forces the charges into a periodic motion at a frequency which depends upon their concentration and mass. Both the electrons and ions can be stimulated into such motion. Another type of oscillation is possible for positive ions in the space where a potential minimum occurs. Such a minimum occurs in the Faraday dark space. The ions are forced into oscillation here much like the electrons are forced into oscillation around the grid of a Barkhausen-Kurz oscillator. Finally, there is the possibility of the discharge current being either choked off or started at periodic intervals.

B. Plasma Oscillations

Tonks and Langmuir (23) were the first to publish theoretical equations for the frequency of plasma oscillations. Following the general method employed by them, it is easy to derive an equation for the natural oscillation frequency of electrons in the plasma. Since the mass of an electron is so small relative to the mass of

an ion, it can be assumed that ions remain practically stationary. The current density due to the motion of the electrons is

$$\mathbf{J} = -nev \quad (1)$$

where n is the number of electrons per cubic meter and v is their velocity in meters per second. Ampere's law becomes

$$\nabla \times \mathbf{H} = \epsilon \dot{\mathbf{E}} - nev \quad (2)$$

Differentiating it with respect to time gives

$$\nabla \times \dot{\mathbf{H}} = \epsilon \ddot{\mathbf{E}} - ne\dot{v} \quad (3)$$

The acceleration \dot{v} can be found from the force equation

$$\mathbf{F} = -e\mathbf{E} - e(\mathbf{v} \times \mathbf{B}) = m\dot{\mathbf{v}} \quad (4)$$

For small oscillations, $\mathbf{v} \times \mathbf{B}$ is small and can be neglected. Making this approximation and substituting equation (4) in equation (3) gives

$$\nabla \times \dot{\mathbf{H}} = \epsilon \ddot{\mathbf{E}} + \frac{ne^2}{m} \mathbf{E} \quad (5)$$

but

$$\nabla \times \mathbf{E} = -\mu \dot{\mathbf{H}}$$

hence

$$\nabla \times \dot{\mathbf{H}} = - \frac{\nabla \times (\nabla \times \mathbf{E})}{\mu}$$

and

$$- \frac{\nabla \times (\nabla \times \mathbf{E})}{\epsilon \mu} = \ddot{\mathcal{E}} + \frac{ne^2}{\epsilon m} \mathcal{E} \quad (6)$$

When the portion of electric field due to $\dot{\mathbf{H}}$ is negligible, $\nabla \times \mathbf{E}$ can be set equal to zero, and equation (6) becomes

$$\ddot{\mathcal{E}} + \frac{ne^2}{\epsilon m} \mathcal{E} = 0 \quad (7)$$

which is the equation for simple harmonic motion at a frequency of

$$f = \frac{1}{2\pi} \left(\frac{ne^2}{\epsilon m} \right)^{\frac{1}{2}} \quad (8)$$

Substituting numerical values for the charge e and the mass m of an electron together with the dielectric constant ϵ reduces this equation to

$$f = 8.98 n^{\frac{1}{2}} \quad (9)$$

When $\nabla \times \mathbf{E}$ is not zero, it is necessary to recall that the displacement of δn charges per unit volume would give rise to a potential gradient

$$\nabla \cdot \mathcal{E} = \frac{\delta n}{\epsilon} \quad (10)$$

Taking the gradient of equation (6) would make the left side zero and reduce the right side to a form like equation (7) with \mathcal{E} replaced by δn . Consequently the frequency would be the same. Two alternative derivations for this frequency are given by Seeliger (20).

The waves described above are not propagated through the plasma. This is shown by the absence of space coordinates in equation (7) which indicates that the group velocity is zero and that the wave moves continuously in a fixed region. However, the existence of certain factors may allow transfer of energy from the disturbance. The electrons involved may be moving as a body through the plasma, or a local oscillation may be traversed by a fast electron beam which would be rhythmically accelerated or retarded. Perhaps the most important factor in setting up external fields is the probable occurrence of unsymmetrical oscillations.

The derivation for the frequency of ion oscillation is not as simple as that for electron oscillation. It is complicated by the fact that the motion of the electrons as well as of the ions must be considered. The net charge displacement is equal to the difference between the ion and electron displacement. The differential equation for the oscillation is obtained by combining this equation

with the equation of motion. The resulting form is difficult to solve, but a qualitative idea of the frequency behavior can be had by assuming the solution in the form of an infinite train of plane parallel waves. The resultant expression for frequency reduces to equation (8) by allowing an additive term in the denominator to approach zero. In other words, the frequencies arising from ion oscillations are generally less than the value indicated by equation (8) but approach that value as an upper limit. Since m in this case represents the mass of an ion, the highest possible frequency for ionic oscillation is less than that for electronic oscillation by a multiplying factor which is equal to the reciprocal of the square root of the ratio of the mass of an ion to that of an electron.

Linder (14) showed that the forces arising from electron gas pressure should have been taken into account in the derivation of the basic equation for electronic oscillation. The displacement of the electronic charge gives rise to pressure gradients as well as electric gradients, and these must be included in the equation of motion if a true picture is to be obtained. The addition of this correction term shows that a whole series of oscillation frequencies are possible which have as their

lower limit the value given by equation (8). Experimentally the series appears as a continuous band due to the breadth of the individual frequencies and the closeness of their spacing. The upper frequency limit of the band is 2.14 times the lower limit. These results are in agreement with the experimental data where bandwidths of the order of one octave were observed.

Adirovich (1) (2) combined the kinetic equation with a macroscopic description of the interaction between volume charges. Collisions and disturbing influences were neglected. The problem was assumed to be one-dimensional with a Maxwellian distribution when in the stationary state. The results indicate that a spectrum of frequencies occur extending from zero to 1.284 times the value given by equation (8). For the range below the frequency of equation (8), there are two solutions for each possibility. One represents a variable surface polarization of the plasma and the other a wave. Above the frequency of equation (8), both are of the wave form.

C. Oscillations in a Potential Minimum

A study of oscillations of a hot-cathode glow discharge in argon was made by Fox (5). At very low pressures, it was found that the radio-frequency output was

very noisy and the glow feeble. When the pressure was increased to about 0.1 millimeters of mercury, the light from the tube suddenly increased and oscillatory output settled down to steady discrete radio frequencies. The frequencies observed seemed to be harmonics of a fundamental which decreased in frequency with an increase in pressure.

When a magnet was placed near the Faraday dark space, the regular oscillations disappeared and the output became noisy. This performance suggested that the oscillations probably arose from a periodic motion about the potential minimum which occurs at the Faraday dark space. A slow-moving ion on arriving there could conceivably be trapped and oscillate for a time until it acquired sufficient energy to get over the hump on the cathode side. The presence of the magnetic field would supply an additional force which could upset the regularity of the motion and account for the noise which was observed to replace the normal oscillation. The decrease in frequency with increase in pressure could also be accounted for by the larger number of collisions which an ion would make while in the Faraday dark space and the consequent greater tendency to slow down its motion. The presence of

harmonic frequencies was ascribed to the presence of irregularities in the shape of the potential minimum.

Cobine and Gallagher (3) attribute some oscillations they observed in an 884 tube to a similar mechanism. These oscillations appeared when the tube was operated at such a low current that the plasma did not exist. Motion of positive ions in the potential minimum at the cathode was considered to be responsible for the phenomena.

D. Periodic Interruption of the Current

Trichel (24) made an oscillographic study of the currents flowing in negative point-to-plane corona in air. He found that the current was composed of discrete pulses similar in form to those of a relaxation oscillator. The shape was independent of the current; but, as the current was increased, the pulses occurred closer together. Consequently, the observed frequency was found to increase in direct proportion to the current flow. The frequency was also found to vary roughly as an inverse function of the radius of the point and as a direct function of the pressure. At some large value of current the periodic discharge disappeared and noisy corona took its place.

Trichel explained the periodic character of the discharge by starting with the positive ions which are formed near the point by external agencies. When the field is sufficiently high, these ions receive enough energy in their last free path to produce at least one secondary electron at the cathode. The electron forms additional ions by inelastic collisions until it reaches a place where the field is no longer great enough to further the process. There it combines with the oxygen molecule to produce a negative ion. In the region where this combination takes place, a negative space charge is gradually built up. Between this region and the point, a spindle-shaped positive ion space charge is accumulated at the same time. This space charge is accelerated toward the point where it greatly increases the field intensity and greatly increases the current flow. A place is eventually reached by the positive space charge where it effectively stops the ionization by collision and causes the current to decrease. This occurs because the distance between the positive space charge and the cathode becomes too short to allow successive ionizing impacts and the field in the region beyond is weakened to such an extent that no ionizing impacts occur there either. As the last positive ions are drawn into the cathode, they produce

secondary electrons which now find themselves in a field strong enough to begin the production of another positive ion space charge and start the cycle anew.

Hudson (11) found that the relaxation pulses observed by Trichel were not produced by discharges from clean smooth points. After the discharge had been running awhile, specks of dust collected on the point and the relaxation pulses began. It was also observed that the Trichel pulses could be started immediately on clean points by dusting them with magnesium oxide powder. These observations prompted him to advance a different theory for the mechanism of the discharge. The small insulating particles on the surface of the point are charged up by the positive ions. At the same time, the accumulation of negative ions sets up an inhibiting field which stops the flow of current. When these inhibiting ions have been swept away, the charged particles on the surface of the cathode initiate the new pulse by producing the necessary electrons. The size of the particles is such that charging them to a relatively low potential produces a gradient near the surface which is great enough to cause high-field emission of electrons. As an alternative, the dielectric strength of the particle may be low enough to break down

in localized places, thus giving rise to the electrons necessary to initiate the discharge.

A process of periodic current interruption in a gas tube which has been put to practical use is described by Kleinwächter (12). If an arc discharge is strongly constricted by a small orifice, the current interrupts itself at high frequency. A high voltage gradient exists through the area of arc constriction; and it together with the high current density leads to intense ionization. Since the positive ions which are formed there are swept out of the area with a greater velocity than the average thermal velocity of the gas molecules, an evacuated region soon develops. This leads to extinction of the arc. As the gas pressure again rises in the constricted area due to diffusion of neutral molecules from the outside, conditions become favorable for the initiation of a new arc and the process is repeated. The frequency of oscillation is equal to the reciprocal of the total time required for this process. It is a decreasing function of both the size of the orifice and the molecular weight of the gas. Conversely, it is an increasing function of the pressure.

Other investigators have also built gas tubes operating on the above principle. The tubes built by Granovsky and Suetin (8) differed from those built by Kleinwächter

in that they used a dielectric rather than metallic diaphragm. This construction eliminated the difficulty experienced with the diaphragm acting as a secondary electrode. Tubes were built which developed powers up to one kilowatt at frequencies ranging from 15 to 100 kilocycles.

With a given tube, it was observed that the current oscillated between zero and a maximum value which increased with an increase in pressure. When a certain pressure was reached, the minimum current was no longer zero but increased at a more rapid rate than the maximum current. Thus the amplitude of oscillations was decreased and a direct-current component was added. With further increase in pressure, a point was reached where the oscillation stopped completely and was replaced by a steady arc current.

E. The Problem

Most of the fundamental studies of oscillations in gases have been made at relatively low pressures on mercury vapor or the inert gases. The work of Trichel is an exception. His studies were closely allied to the radio-interference problem involving discharges from pointed conductors in air such as occurs in precipitation

static or corona from high-voltage installations. For that reason, the work was of practical as well as theoretical interest. However, the effect of the composition of the gas was not investigated by Trichel, and a search of the literature failed to reveal the existence of any such studies on either hydrogen or oxygen. Consequently, a study of these gases was undertaken.

Since the radiated field is responsible for causing interference, it was considered desirable to make measurements on this field directly rather than confine the observations to the discharge current itself as was done by Trichel. Furthermore, it was considered necessary to provide some sort of automatic recording for the received signal strength so that a complete picture of the oscillatory discharge might be obtained. It was felt that precision measurements of the current and voltage were unwarranted because of the erratic character of the discharge. Instead, it was desirable to obtain the greatest possible accuracy that was consistent with speed and convenience in making the observations. The experimental apparatus was set up with these ideas in mind.

II. EXPERIMENTAL APPARATUS

A. General

Experimental apparatus was set up to meet three general objectives. These involved preparing the gases, measuring the pressure of the gas in the tube, and recording the radio-frequency radiation from the discharge. So far as possible it was desirable to use standard, readily available equipment to accomplish these objectives so as to minimize the amount of special construction required.

A general view of the final assembly of the apparatus is given in Fig. 1. The equipment on the right is the glassware for preparing the gases and introducing them into the discharge tube. On the left is the apparatus for measuring the input to the tube and recording its radio-frequency output. The wide-range McLeod gauge at the extreme right of the figure was used as a primary standard for pressure measurement. To the left of this is the mercury-diffusion pump and nitrogen generator followed in turn by the electrolytic hydrogen and oxygen generator. The latter is readily identified by its large beaker of electrolyte which is nearly in the center of the figure. The meter on the right of this beaker is an ammeter to

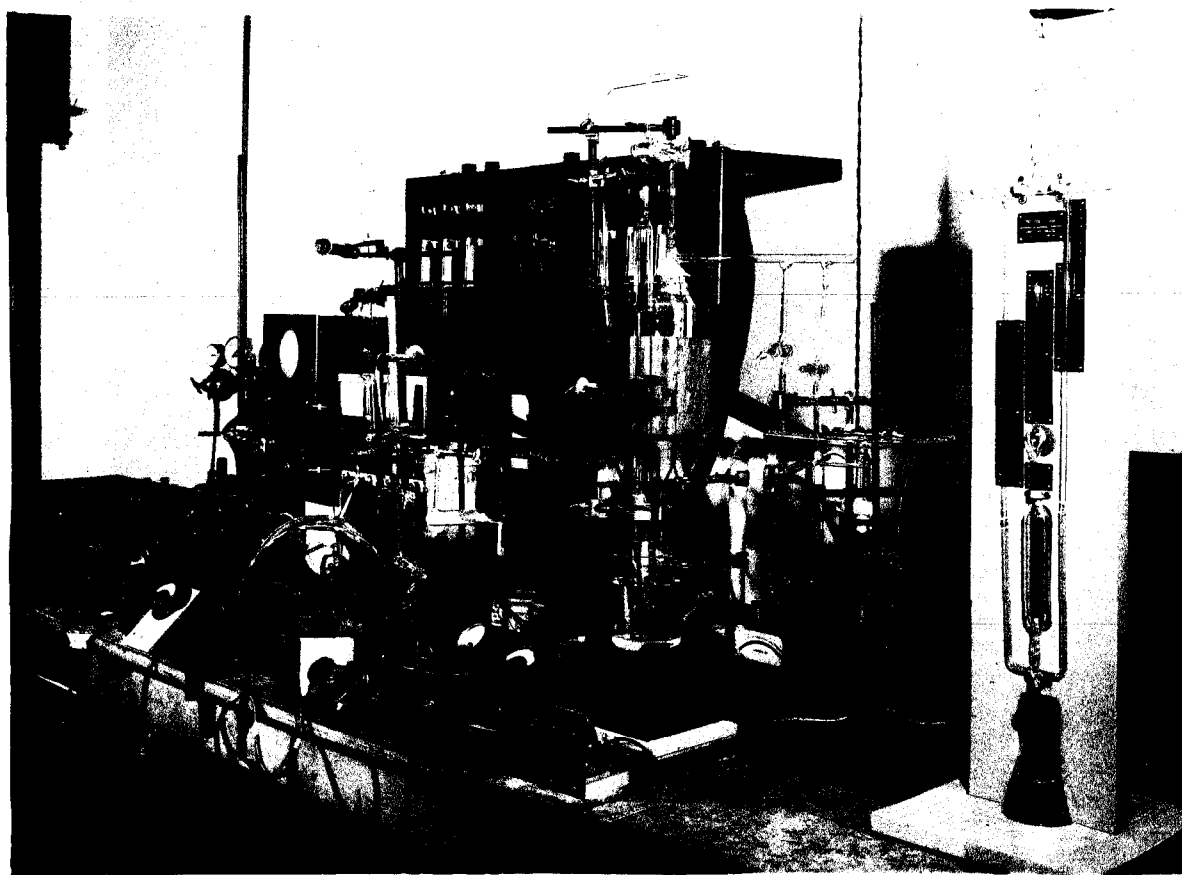


Fig. 1. General view of apparatus.

measure the electrolysis current, and the meters on the left are associated with the Pirani and thermocouple gauges. Just above the latter group of instruments is the P_2O_5 desiccator tube. Immediately behind it is a large beaker of ice water which provided a constant-temperature bath for the Pirani gauge. The thermocouple gauge is just to the left of this. Another thermocouple gauge is attached to the mercury diffusion pump and can be seen slightly to the left of the McLeod gauge, but it was not used during the experiment since it was too far away from the discharge tube to be of practical value. The glass manometer rises above the Pirani and thermocouple gauges and is characterized by the viewing telescope on top. The discharge tube itself is enclosed in the large cylindrical section of wave guide below the glass manometer and can be faintly seen through the copper screen covering the end of this guide. The pick-up probe is also located there. Behind the gauges and wave guide is the radio receiver. On top of it are two Voltchmysts for measuring the current and voltage supplied to the tube from the high-voltage rectifier under the table. The cathode-ray oscillograph which is to the left of the Voltchmysts was used to observe the wave form of the input current. On the extreme left edge of the

figure is the magnetic oscillograph which recorded the output from the radio receiver. The meter in front of it was connected in series with the oscillograph element and gave a visual indication of signal strength. The metal receiving tube above the front end of the magnetic oscillograph is the input to a frequency-calibrating circuit. The power supplies which were necessary for the added circuits lie behind the receiver and oscillograph.

B. Preparation of Gases

Provision was made for preparing hydrogen, oxygen, and nitrogen to a high degree of purity. Hydrogen and oxygen were prepared by electrolysis with nickel electrodes in a 20 per cent solution of potassium hydroxide. Current was supplied by a low-voltage motor-generator set.

According to Engelhardt (4, p. 31) and Taylor (22), the electrolytic process yields hydrogen to a purity of about 99 per cent and oxygen to a purity of about 97 per cent directly. Since the principal impurity in each case is the other constituent of water, it can be removed by combustion in the presence of a catalyst. In the early part of the work, hydrogen was purified by heating a copper filament in the gas to red heat. Later the copper filament was replaced by one of platinum so that it could

be used for the purification of oxygen as well as hydrogen. The purity of both gases prepared by this apparatus is probably in the neighborhood of 99.9 per cent; however, it was not practical to set up analytical equipment to check this point.

Nitrogen was prepared by gently heating a solution of chemically pure ammonium chloride and potassium nitrite in the flask shown in Fig. 2. This flask is designed so that the liquid displaced by the generated gas can flow into an external container. When the stopcock is opened to allow the nitrogen to flow into the system, the liquid is returned and the cycle started anew. The chemical reaction for the process is



Originally it had been intended to study the radio-frequency spectra from nitrogen as well as from hydrogen and oxygen; however, it became apparent as the experiment progressed that it would be wiser to devote more effort to the study of hydrogen and oxygen and forego the study of nitrogen at this time. Consequently, the nitrogen generator was used only in conjunction with the calibration of the pressure gauges to be described in a later section.

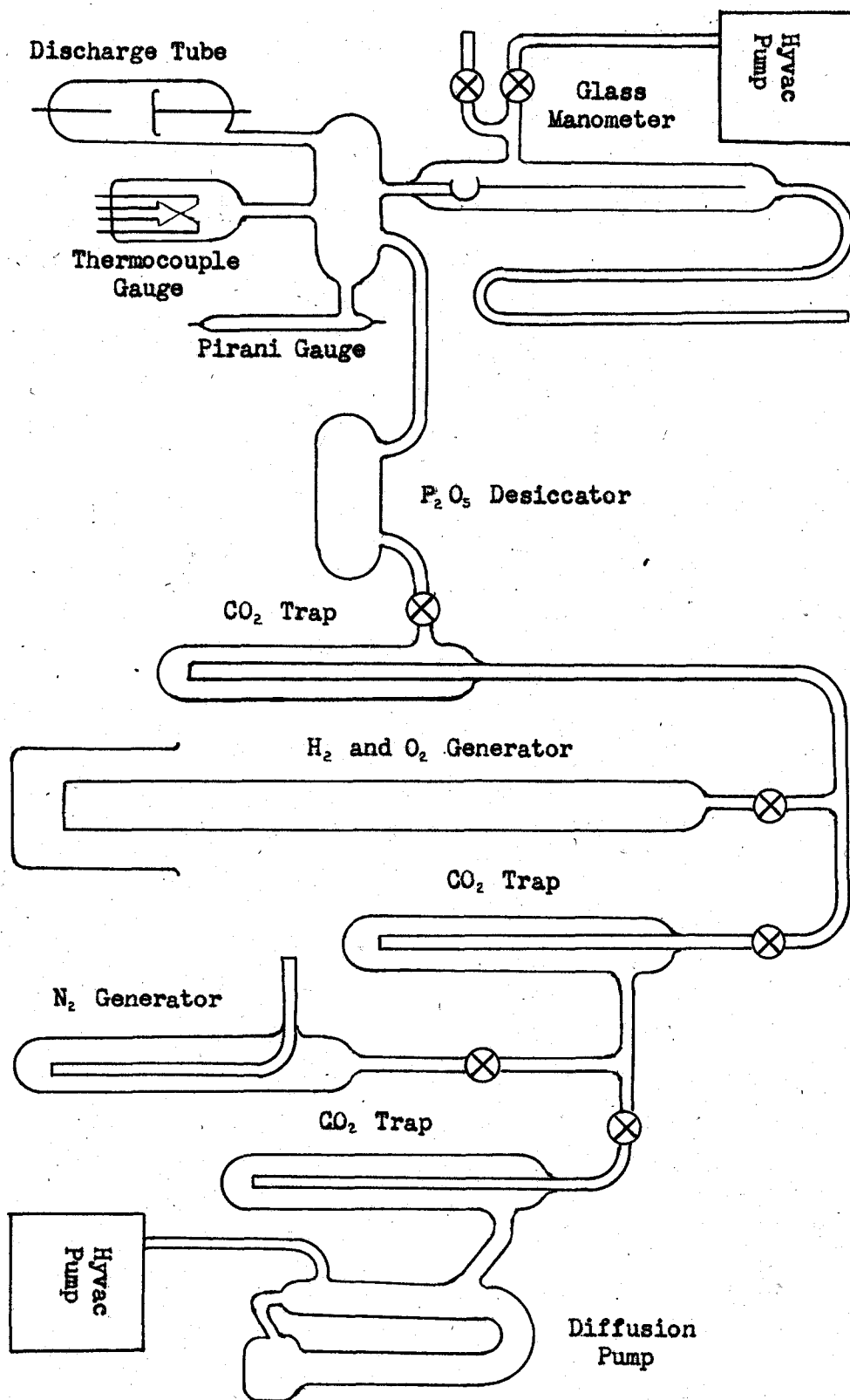


Fig. 2. Schematic diagram of glassware.

Water vapor was necessarily mixed with the end product in all cases. Most of it was removed by the CO₂ traps which were surrounded by a freezing mixture of dry ice and acetone. The P₂O₅ desiccator removed the rest.

Contamination by mercury vapor from the diffusion pump was minimized by proceeding as follows: The tube was baked for more than one hour at a temperature of 350°C while connected to the highest possible vacuum (better than 10^{-4} millimeters of mercury). At the end of this time, the stopcocks leading to the pump were turned off and the tube cooled. The purified gas was then gradually added. Sometimes during the baking-out processes a small amount of hydrogen was admitted to the tube to reduce any oxides which may have formed on the electrodes. The stopcocks to the pumps were opened again and the pumping process resumed under the conditions described above.

It will be noted that there are several traps between the tube and the diffusion pump. This was to insure that any mercury vapor which could be removed by the freezing mixture would be removed. To assist in this process the trap adjacent to the discharge tube was cleaned from time to time by closing the stopcock between it and the tube, and heating it while drawing a high vacuum on the system.

C. Discharge Tube

Figure 3 shows the constructional detail of the discharge tube. Essentially it consists of a needle point a short distance from a plane surface. The point was made from 40-mil tungsten wire conically ground to enclose an angle of approximately 30 degrees. It was chosen rather than a small wire ground with a spherical end because the former produces more corona with a given voltage than the latter. The voltage output from the available power supply was limited to 10 kilovolts making this choice necessary. Unfortunately the voltage-current characteristic of a needle point is not nearly as stable as that of a small spherical point (26) and data on it can only be checked to a fair degree of accuracy. However, this disadvantage was overshadowed by the fact that with a given input a considerably greater radio-frequency output could be expected.

The size of the plane was limited by the size of tubing which could be conveniently worked with laboratory glassblowing equipment. It was mounted on a screw thread so that the distance between it and the point could be adjusted to a high degree of precision. A small bar of soft iron perpendicular to the threaded collar provided an armature which could be turned by means of external

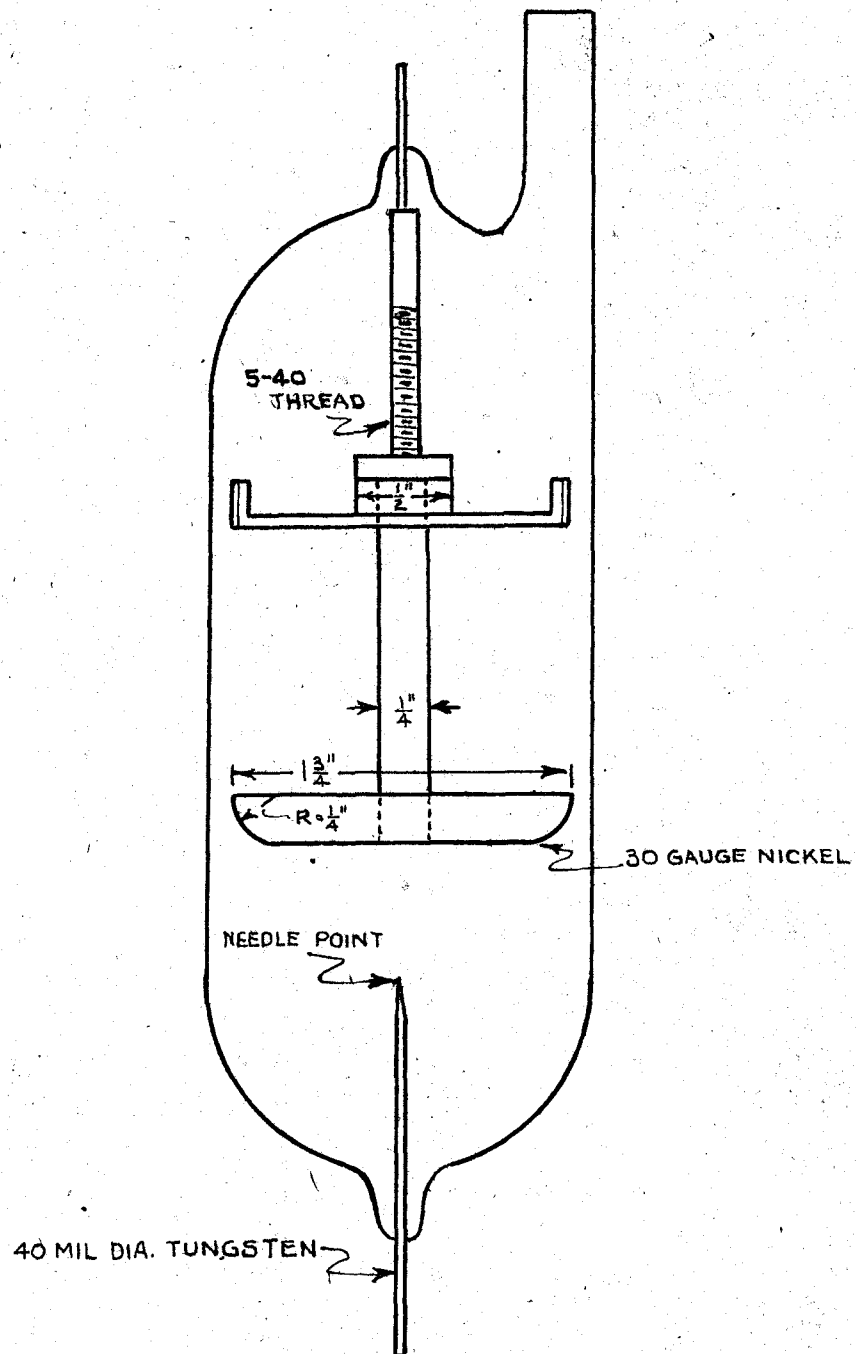


Fig. 3. Constructional details of discharge tube.

magnets. A pair of Alnico magnets mounted on a board proved satisfactory for this purpose. Figure 4 is a photograph of the finished tube together with its adjusting magnets.

Initially it was intended to use this adjustment for the purpose of investigating the effect of spacing on the radio-frequency output. However, this phase of the problem was not studied because the results which were obtained indicated that the effect if any would probably be obscured. Consequently, the spacing was adjusted to 38 turns or 0.95 inches and left there.

D. Measurement of Pressure

It was desirable during the course of the experiment to measure pressures all the way from atmospheric to high vacuum. No one gauge could satisfactorily cover this range and so several gauges were used to cover different portions.

A mercury manometer would ordinarily be considered a satisfactory instrument for measuring pressures near atmospheric. However, it was not suitable for this experiment since it would have given an exposed mercury surface connected to the gas tube and led to contamination. The glass manometer described by Wright (25) provided a means

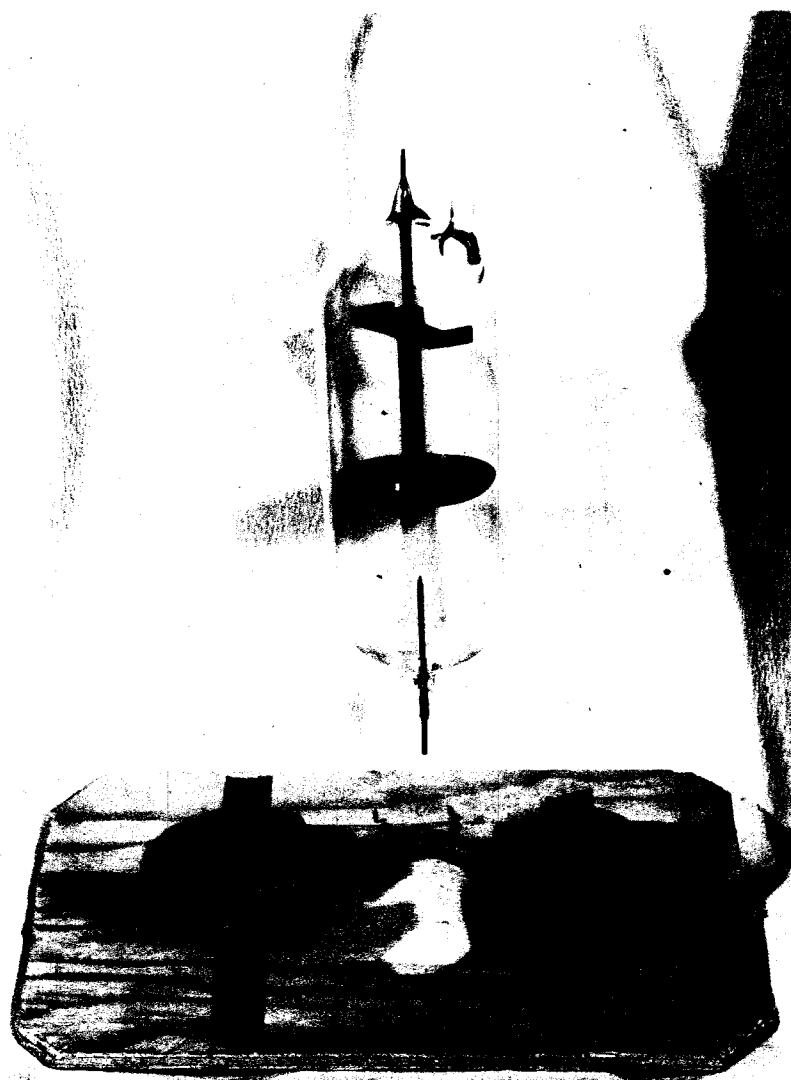


Fig. 4. Discharge tube together with magnets for adjusting spacing.

of getting around this difficulty. Essentially this instrument consists of a glass Bourdon tube connected to the vessel where pressure is being measured and surrounded by a jacket, which in turn is connected to a mercury manometer. The Bourdon tube thus provides a flexible glass member between the vessel and the manometer. By admitting or removing air from the surrounding jacket, the pressure in it can be adjusted to the pressure in the tube and read directly on the manometer. The motion of the Bourdon tube is magnified by a long glass fiber attached to its upper edge. The tip of the fiber is observed with a telescope and brought into alignment with a cross hair for pressure balance.

With the least sensitive Bourdon element constructed during the course of this work, it was possible to take a succession of independent readings where the maximum deviation from the mean value was less than 3 millimeters of mercury. But, this error was not the limiting factor in the application of the gauge used. It was observed that there was sometimes relative motion between the telescope and the gauge, thus displacing the zero reference point. By independent checks of pressure at atmospheric and high vacuum, this error was found to be of the order of 5 millimeters of mercury. Consequently, pressure readings are in doubt by

this amount. To emphasize the existence of this uncertainty, they are only given to the nearest 5 millimeters.

The gauges described by Wright (25) used a stationary glass fiber attached to the enclosing jacket as a reference instead of the telescope crosshair described above. All attempts to insert such a fiber and line it up exactly failed. This led to the adoption of the telescope method. Since the completion of the experimental work, a technique has been thought out whereby the reference fiber would be attached to a handle allowing it to be moved precisely into position before the glass cooled. With the use of this technique and a sensitive Bourdon element, it should be possible to construct a glass manometer which would be consistently accurate to better than one millimeter.

A McLeod gauge was built following the design of Reiff (17) for use as a primary standard in the low-pressure region. The gauge built was capable of measuring pressures from 2×10^{-5} to 10 millimeters of mercury. The wide range was made possible through the use of index marks on the 100 cubic centimeter compression chamber which divided it into decades having volumes of 10, 1, 0.1 and 0.01 cubic centimeters together with some smaller divisions. By adjusting the level of mercury to an index mark,

it was possible to read the pressure directly on a metric scale beside one of the run-around tubes. Mercury was moved in and out of the compression chamber by connecting the reservoir to atmospheric pressure or vacuum by means of stopcocks.

Experience with the gauge showed that it would have been better to make its overall length great enough to prevent the mercury from rising beyond the start of the compression chamber with atmospheric pressure on the reservoir and high vacuum on the gauge. There are three major advantages to making this change. (1) The gauge could be left connected to the vacuum system at all times without danger of trapping air in the compression chamber during the evacuation process and consequent difficulty in removing it. (2) The gauge could be used as a manometer. Consequently, the range would be extended from the present 10-millimeter limit to atmospheric pressure. (3) Mercury would be moved into the compression chamber by compressed air rather than out of it by a vacuum. Since compressed air is a more readily available laboratory service, this would give added convenience in operation.

Considerable difficulty was experienced with the mercury sticking to the capillary tubing. The sticking was so tenacious at times that the gauge had to be dismantled.

This difficulty was entirely eliminated by grinding the inside surface of the capillaries in accordance with the suggestion of Klemperer (13) and Rosenberg (19).

For the actual measurement of low gas pressures in the discharge tube, it was desirable to have a gauge which was relatively simple to use and which would not contaminate the gas. For this purpose a Pirani gauge of the general type described by Rittner (18) was built. The active element was a 1.5-mil tungsten wire threaded through a 5-inch length of capillary tubing. The wire was spot-welded by the discharge from a condenser to short strips of sheet nickel and thence to heavier tungsten wires used as lead-ins. As shown in Fig. 7, this element made up one arm of a Wheatstone bridge. The gauge was operated by measuring the current which had to be supplied to the bridge in order to bring it into balance. The resistance of the gauge constructed was 5.80 ohms at 21°C. The bridge balanced when this resistance rose to 7.91 ohms corresponding to a temperature of 91.5°C. The galvanometer had a critical damping resistance of 7 ohms so that it was ideal for use in the circuit.

Calibration was made with four different gases by means of the McLeod gauge. The results are presented in Fig. 5. Bulb temperature was maintained at 0°C by means

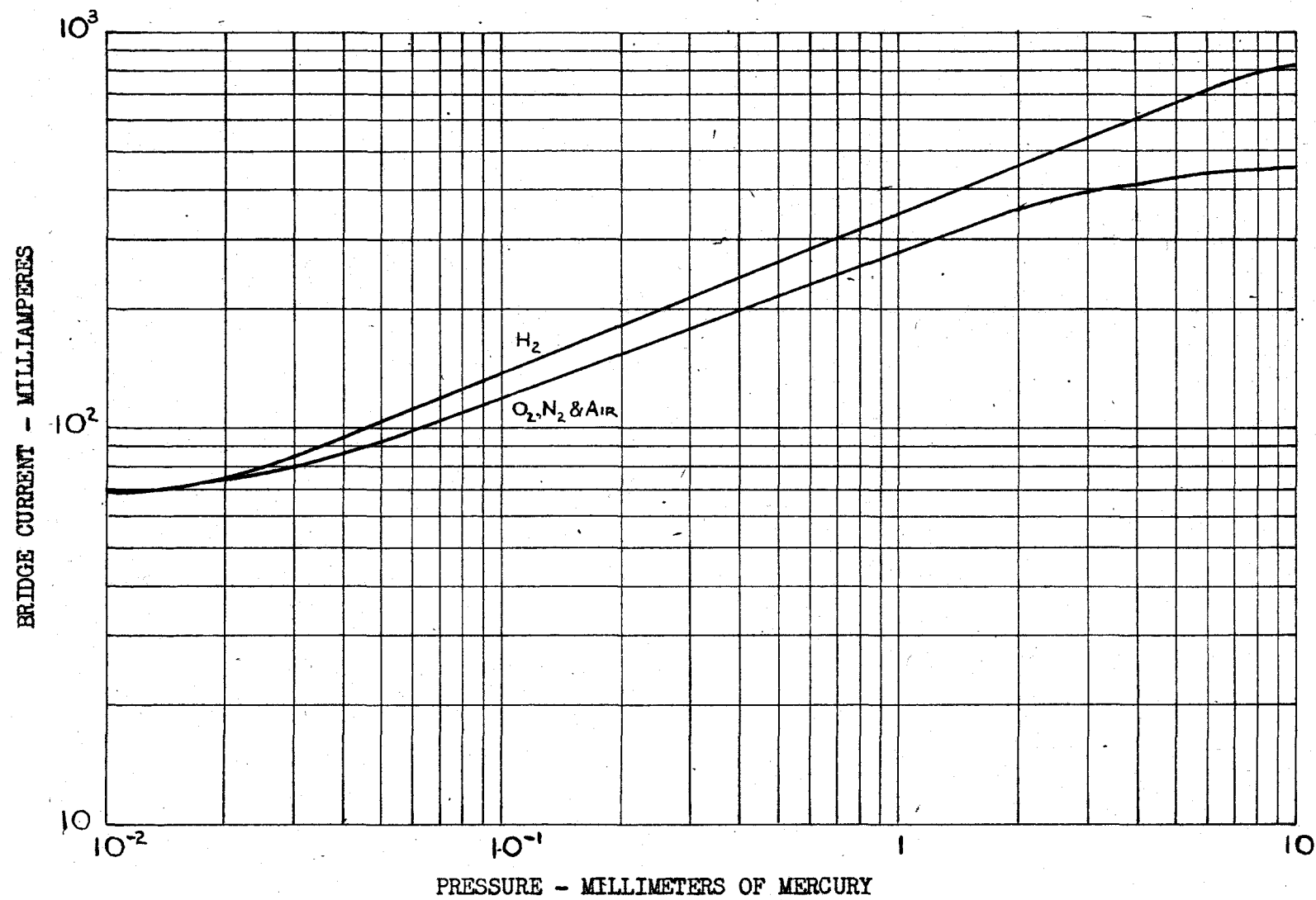


Fig. 5. Calibration curve for Pirani gauge. Bulb temperature 0°C .

TABLE 1

Calibration of Pirani Gauge

Oxygen		Hydrogen		Air	
Pressure mm Hg	Current ma	Pressure mm Hg	Current ma	Pressure mm Hg	Current ma
7.8	458	9.8	810	3.2	395
5.1	427	7.7	800	1.6	335
3.6	400	5.8	720	8.7×10^{-1}	265
2.5	375	4.5	640	4.7×10^{-1}	215
2.0	350	3.3	570	4.1×10^{-1}	200
1.4	312	1.6	425	2.8×10^{-1}	170
1.0	275	8.0×10^{-1}	315	2.3×10^{-1}	160
8.0×10^{-1}	252	3.9×10^{-1}	230	1.5×10^{-1}	140
6.5×10^{-1}	237	3.2×10^{-1}	215	1.3×10^{-1}	130
5.4×10^{-1}	220	2.1×10^{-1}	175	8.1×10^{-2}	110
4.5×10^{-1}	202	8.0×10^{-2}	125	4.9×10^{-2}	93
3.5×10^{-1}	185	6.1×10^{-2}	115	3.4×10^{-2}	84
3.0×10^{-1}	172	4.2×10^{-2}	100	2.1×10^{-2}	76
2.2×10^{-1}	157	2.3×10^{-2}	80	1.3×10^{-2}	70
1.5×10^{-1}	131	1.4×10^{-2}	73		
10.4×10^{-1}	121	1.2×10^{-2}	70		
8.7×10^{-2}	115				
7.0×10^{-2}	107				
5.6×10^{-2}	96				
4.6×10^{-2}	91				
3.6×10^{-2}	84				
3.3×10^{-2}	81				
2.5×10^{-2}	76				
2.0×10^{-2}	73				
1.6×10^{-2}	70				
1.3×10^{-2}	66				

of a bath of ice water. The performance of the gauge under these conditions was extremely reliable. Several independent checks were made on the data with the result that practically no variations in the indicated reading were found. As can be seen from the trend of the curves presented in Fig. 5, the gauge as constructed had a useful range from 10^{-2} to 10 millimeters of mercury.

While the Pirani gauge was extremely reliable in its operation, it was not the most convenient instrument for ordinary use because it had to be adjusted for each reading. Consequently, a direct-reading gauge was provided so that the evacuation process could be quickly checked. A commercial thermocouple gauge sold by the Central Scientific Company was employed for this purpose. It was calibrated the same as the above with the results shown in Fig. 6. The asymptote approached by the curves on the left was subject to variations by as much as 5 microamperes. Most of this variation was found to be due to changes in the ambient temperature. The construction of the gauge was such, however, that it was difficult to provide a constant-temperature bath. Consequently, it was not used for precision measurements.

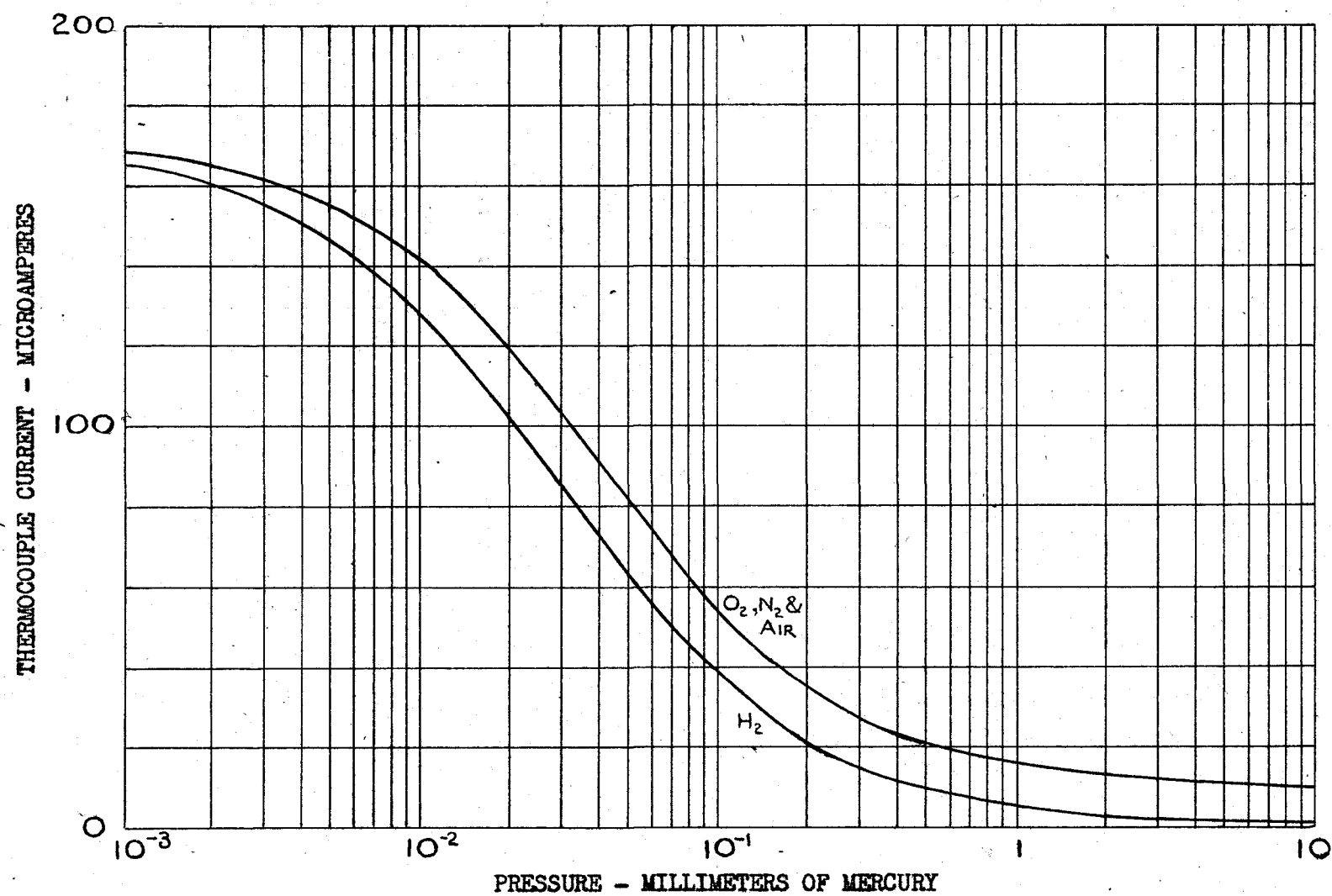


Fig. 6. Calibration curve for thermocouple gauge. Heater current 25 ma. Ambient temperature $26^{\circ}C$.

TABLE 2

Calibration for Thermocouple Vacuum Gauge
Using a Heater Current of 25 Milliamperes

Oxygen		Hydrogen		Air and Nitrogen	
Pressure mm Hg	Thermo- couple Current μ a	Pressure mm Hg	Thermo- couple Current μ a	Pressure mm Hg	Thermo- couple Current μ a
7.8	10.0	7.7	1.0	(Air)	
5.1	10.2	3.4	2.0		
3.6	10.8	1.6	3.6	6.0×10^{-2}	72.0
2.5	11.2	1.7×10^{-1}	24.5	4.8×10^{-2}	79.7
2.0	12.0	1.4×10^{-1}	29.0	3.85×10^{-2}	90.0
1.4	13.0	1.1×10^{-1}	38.0	3.2×10^{-2}	97.5
1.0	14.2	6.0×10^{-2}	53.0	2.5×10^{-2}	109.2
8.0×10^{-1}	16.7	4.0×10^{-2}	70.0	1.8×10^{-2}	122.0
6.5×10^{-1}	18.0	3.1×10^{-2}	83.0	1.1×10^{-2}	138.5
5.4×10^{-1}	20.0	2.3×10^{-2}	96.0	4.85×10^{-3}	154.0
4.5×10^{-1}	22.0	2.0×10^{-2}	102.5	3.0×10^{-3}	161.0
3.5×10^{-1}	25.8	1.7×10^{-2}	111.0		
3.0×10^{-1}	28.2	1.3×10^{-2}	120.5		
2.2×10^{-1}	34.0	1.1×10^{-2}	125.5		
1.5×10^{-1}	46.0	7.9×10^{-3}	134.0		
10.4×10^{-2}	52.8	7.0×10^{-3}	137.5	(Nitrogen)	
8.7×10^{-2}	59.5	6.1×10^{-3}	140.5		
7.0×10^{-2}	67.5	5.8×10^{-3}	142.5	3.8×10^{-1}	23.0
5.6×10^{-2}	77.0	4.9×10^{-3}	147.0	1.7×10^{-1}	40.0
4.6×10^{-2}	84.5	4.7×10^{-3}	147.5	7.2×10^{-2}	62.5
3.6×10^{-2}	94.8	4.0×10^{-3}	151.0	3.8×10^{-2}	90.0
3.3×10^{-2}	100.0	3.7×10^{-3}	152.5	2.05×10^{-2}	117.0
2.5×10^{-2}	111.5	2.9×10^{-3}	155.0	6.3×10^{-3}	150.0
2.0×10^{-2}	119.2	2.3×10^{-3}	159.5	2.6×10^{-3}	163.5
1.6×10^{-2}	127.0	1.7×10^{-3}	162.0		
1.3×10^{-2}	136.5	1.2×10^{-3}	165.0		
8.6×10^{-3}	144.0				
7.0×10^{-3}	148.5				
4.8×10^{-3}	155.5				
2.4×10^{-3}	164.0				

E. Pick-up Probe and Receiver

Interference from radio stations made field measurements of the radiation from the discharge tube virtually impossible. It was necessary to devise a means for making the measurements inside a shielded area. The use of wave guides of smaller than critical size for the construction of signal-generator attenuators by Harnett and Case (9) and the development of the theory of their operation by Linder (15) suggested the possibility of such an arrangement for this case. The discharge tube was mounted at one end of a 10-inch diameter pipe and a pick-up device was mounted at the other end. With precision construction it would be possible to accurately determine the strength of the field being generated by knowing the strength of the signal being received and the spacing between the pick-up device and the source. However, such construction was not justified for the present work because qualitative rather than precise quantitative results were being sought.

Two forms of pick-up probe were used during the course of the experiment. The first of these was a 5-turn coil 1-inch in diameter connected between the grid and cathode of the 6J7 tube shown in Fig. 7. This coil

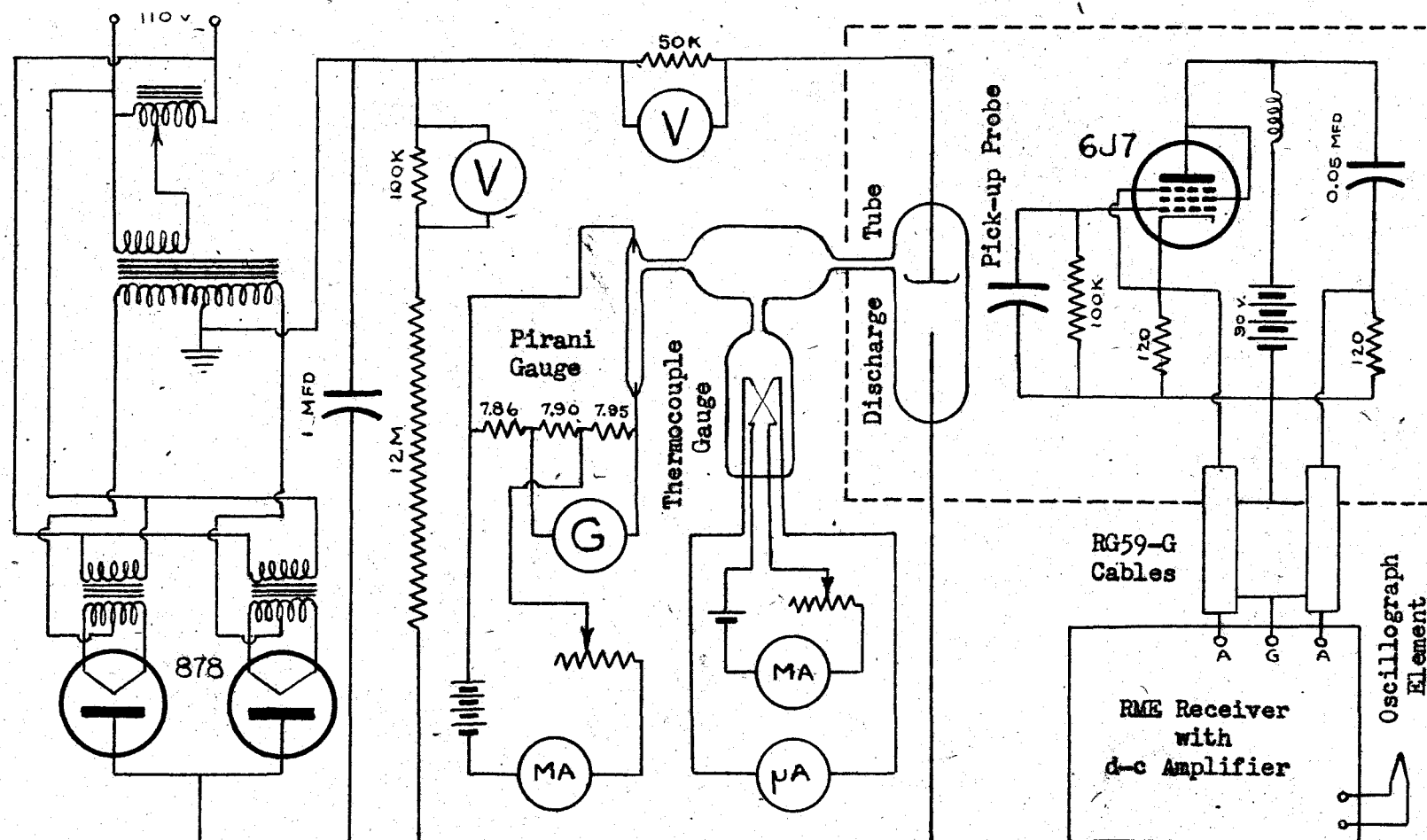


Fig. 7. Schematic diagram of general electrical connections including the circuit diagram of the pick-up probe.

was a complete failure. The non-performance of this device was not at all surprising when it was later found that practically all of the radiated energy was in the low-frequency range. The impedance of the coil was so low that no appreciable voltage was developed across it. The number of turns had been limited to insure that the coil could not operate near its natural frequency and would be truly aperiodic in performance.

Following the failure of the coil as a pick-up device, it was suggested that an electrostatic pick-up be tried. Accordingly a 0.1-megohm resistor was paralleled with a condenser consisting of a pair of square plates 3 centimeters on edge spaced 1 centimeter apart, and this combination was connected between the grid and cathode of the input tube as indicated on the diagram. Its performance was entirely satisfactory, and it was used for all of the tests which were made. Figure 8 is a photograph of this probe.

The input impedance to the doublet antenna terminals of the RME receiver varies from 150 to 450 ohms over its tuning range with an average value near 300 ohms. In order to match this impedance to the pick-up probe and at the same time provide an input which was balanced with respect to ground, the circuit shown in Fig. 7 was

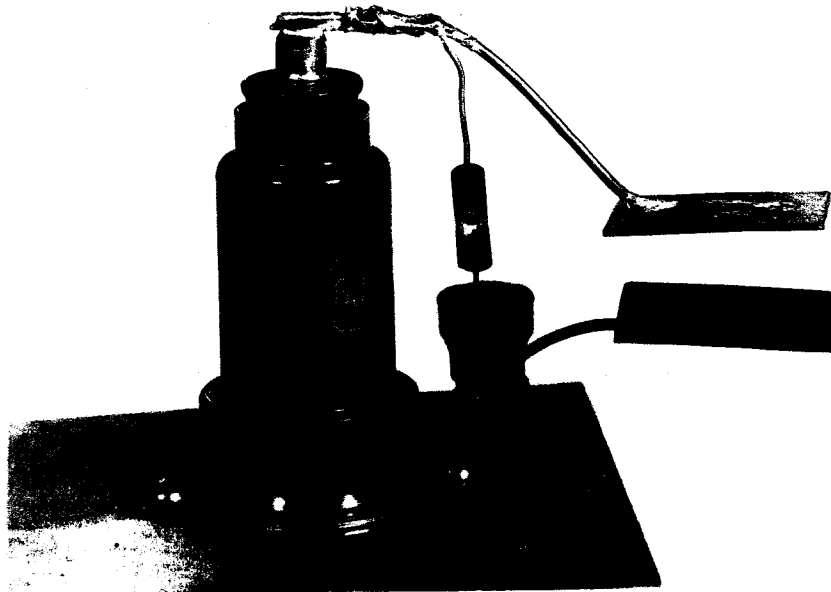


Fig. 8. Pick-up probe.

employed. The circuit is related to the cathode follower but differs from it in that a balanced output is provided.

No changes were made in the receiver itself up to and including the second detector. From this point on, it was necessary to make modifications to provide a relatively heavy current output which was proportional to the received signal strength rather than to use the normal audio-frequency output.

The automatic-volume-control voltage developed by the second detector supplied a convenient source of potential which varied from zero volts with no signal to approximately -10 volts with a very strong signal. The oscillograph element which was to record the signal strength required a current of approximately 100 milliamperes to give a satisfactory deflection. When the 6F6 output tube was operated as a triode with 300 volts on its plate, a 0-125 milliampere plate current variation could be obtained with a grid voltage variation from zero to -50 volts. Consequently, a stage of direct-current amplification between the automatic-volume-control output and the 6F6 grid was necessary.

Rather than floating the final stage at a relatively high potential with respect to ground and have the attendant problems of separate heater supply for the 6F6, the

direct-current amplifier design suggested by Ginzton (6) was adopted. From the above analysis, the gain required by the stage was found to be approximately five. Consequently, a 6J5 was chosen as being an appropriate tube for the purpose and the circuit shown in Fig. 9 was evolved. Essentially the coupling circuit consists of a tapped voltage source and a voltage divider with the elements so proportioned that the point c is at the proper positive potential with respect to ground at the same time that the point d is at the proper negative potential with respect to ground.

Ginzton made an analytical solution of this circuit and arrived at a set of design equations for it, but these equations were not at all suited for the present purpose since they assume small signals. Instead the graphical solution shown in Fig. 11 was worked out.

For the present problem, the tube involved was a 6J5 and so its plate characteristic curves were plotted as shown in the figure. It was desirable to use the receiver plate-supply voltage for E_{ap} ; hence, this value was fixed at 280 volts. All the other parameters could be varied at will, but it was desirable to keep E_{ag} as small as possible and necessary to keep R_g below 0.1 megohm.

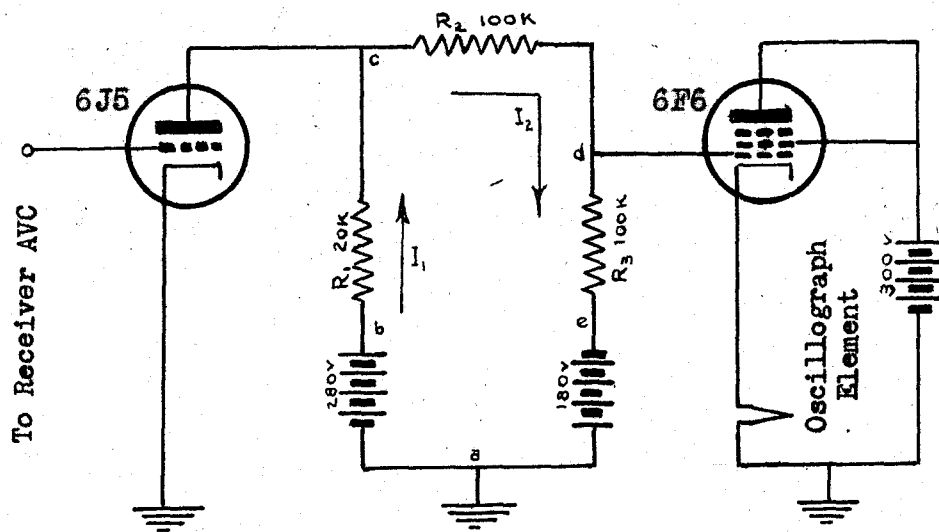


Fig. 9. Direct-current amplifier.

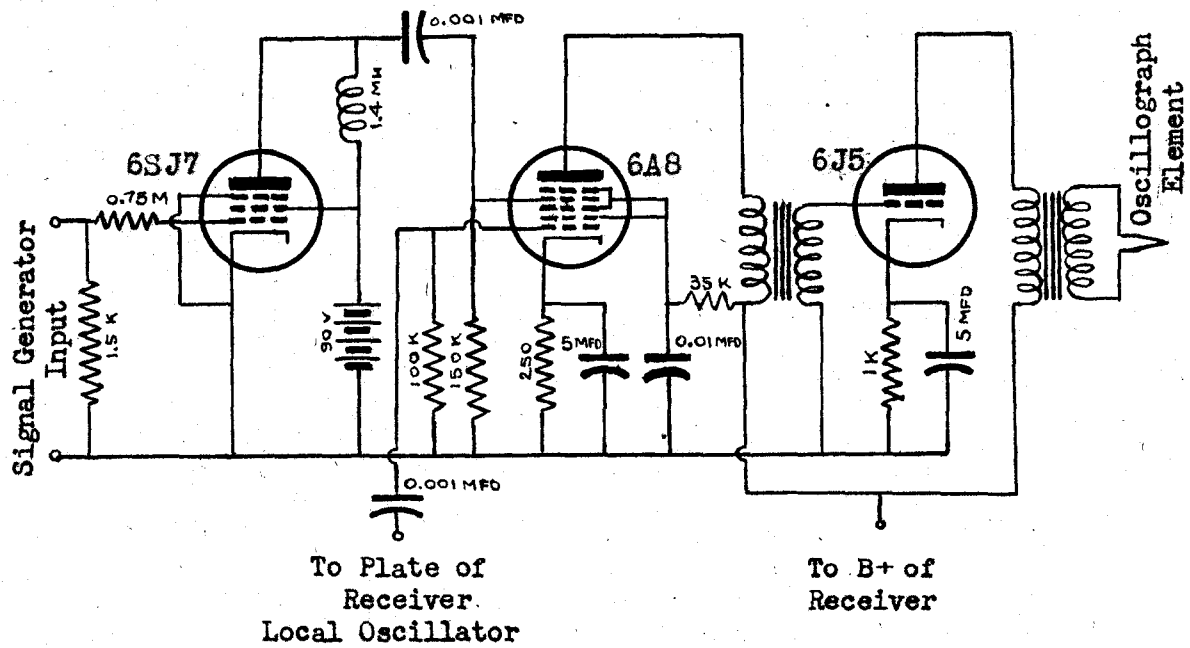


Fig. 10. Frequency calibrating circuit.

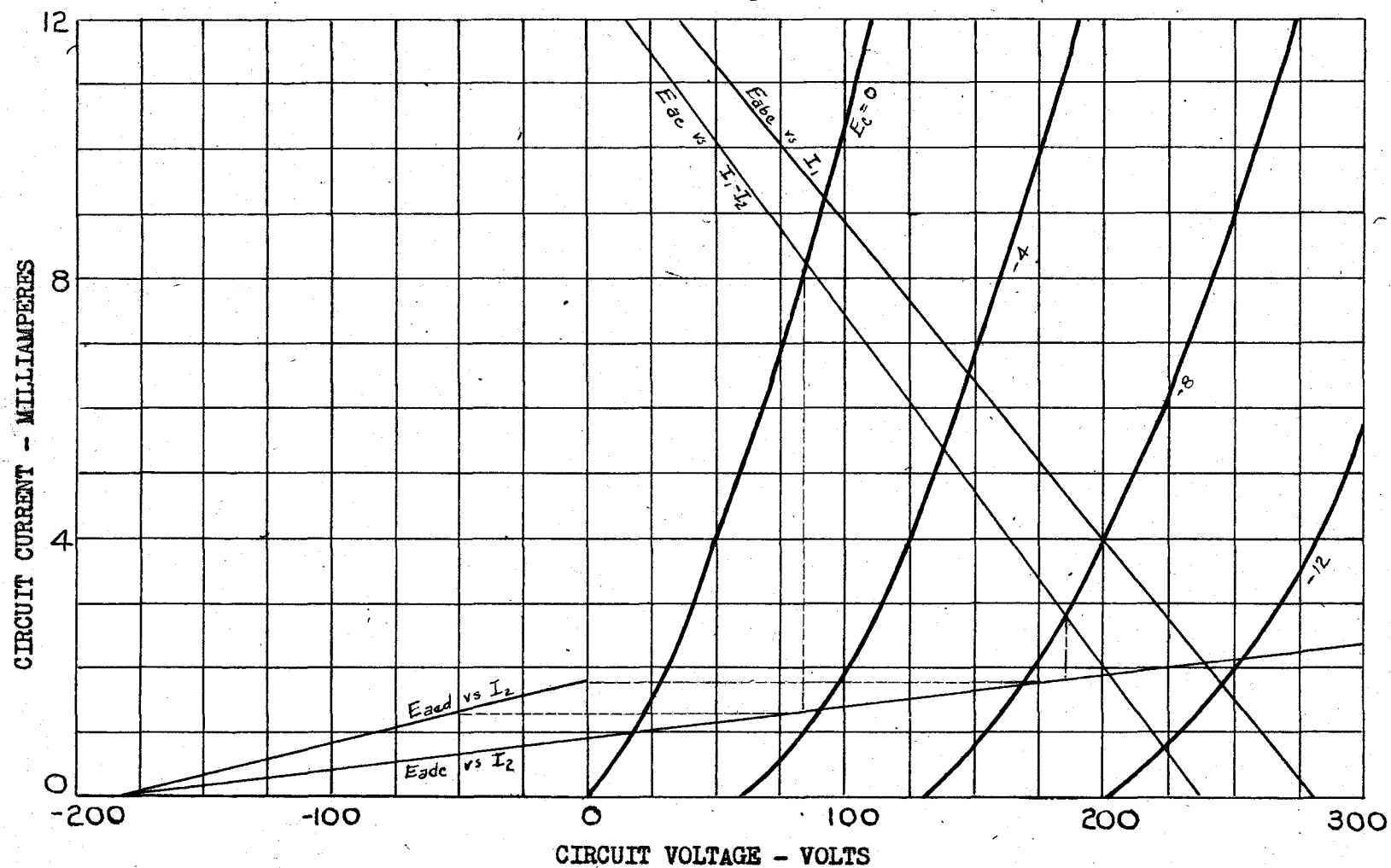


Fig. 11. Graphical analysis of direct-current amplifier.

The line representing the voltage rise E_{abc} as a function of the current I_1 corresponds to the usual load line. Around the other portion of the circuit we have the voltage rise E_{edc} as a function of the current I_2 . In Fig. 11 this line is drawn for a value of E_{ac} corresponding to -180 volts. The difference between these two lines E_{ac} vs. $I_1 - I_2$ represents the voltage at the plate of the tube as a function of the current taken by it. The intersections of this line with the plate characteristic curves give the resultant plate voltages corresponding to various values of grid bias. The projection of them on the E_{edc} vs. I_2 line gives the variation of the current I_2 , and projection of it on the E_{ead} vs. I_2 line gives the voltage variation being applied to the grid of the next tube in line.

The result of changing the parameters of the circuit can easily be seen on this diagram. With the other elements remaining constant, increasing R_1 tends to increase the output, but the gain possible in this direction is limited by the curvature of the characteristic curves and the relatively greater influence of subtracting the E_{edc} vs. I_2 line. In fact if too large a value were selected for R_1 , the existence of this line would cause the tube

to cut off at a relatively low grid bias. A consideration of these factors indicated that 20,000 ohms was near the optimum value for R_1 .

Similarly, it can be seen that if the sum of R_2 and R_3 were made too small, there is also the possibility of early cutoff by the tube. For example, in Fig. 11, if this sum were 100,000 ohms (that is, line E_{a2} vs. I_2 extended), the tube would cut off at -12 volts. On the other hand, large values for this sum would give small variations in the current I_2 and consequent small variations in the bias on the next stage.

Two criteria had to be fulfilled in the selection of R_3 in addition to the size limitation mentioned before. It had to be large enough so that with the available change in I_2 an adequate change in the grid bias on the second tube would be obtained. At the same time it was desirable to have the bias on the 6F6 near zero at the maximum bias expected on the 6J5 so that during operation the grid of the 6F6 would not become positive. Other factors remaining the same, a reduction in the magnitude of E_{a2} would put the operation in the positive region. A change in the magnitude of R_2 and R_3 could put the operation back in the negative region but the range of the variation in bias on the second tube would then be reduced. In order

to get satisfactory operation with this circuit, it was necessary to make E_{ac} equal to -180 volts. A larger voltage would have permitted an increase in the range of operation but the improvement in this direction was not sufficient to warrant its use. The constants of Fig. 9 gave the optimum performance of the circuit.

F. Recording Mechanism and Auxiliaries

A General Electric Type PM-10-A1 magnetic oscillograph was employed as the recording mechanism. It contained several elements which could be used to record other variables in the circuit along with the strength of signal.

The recordings were made on Haloid paper 3 5/8 inches wide. This paper was economical and at the same time sufficiently fast for the present purpose.

Two film holders were provided with the oscillograph--the magazine film holder and the continuous-drive film holder. The continuous-drive film holder was used at first because it offered the possibility of longer records. The added length later proved to be no advantage and so the magazine film holder was adopted.

With the use of the continuous-drive film holder, a means for identifying the frequencies being received

had to be devised. Two schemes were employed, each involving the use of another oscillograph element. One of these simply connected the element in series with a battery and a key. As the dial of the receiver passed 20-degree interval marks, the key was depressed. When the dial reached 80 degrees, the key was depressed and held until it passed 90 degrees. Both a mechanical and a hand contactor were tried in calibration, but both were so erratic in their performance that they were abandoned.

A typical recording for this type of operation is shown in Fig. 13a (page 55). The top trace is proportional to the signal strength being received (that is, the plate current of the 6F6 tube). The next trace is the zero axis for the 6F6 plate current. It will be noted that in this and subsequent recordings that the zero signal strength line lies above the zero current axis. The circuit was purposely adjusted to operate in this manner so that a continuous check on its performance could be made. The last trace is from the calibration circuit.

The other calibrator employed the circuit shown in Fig. 10 (page 41). A standard frequency signal was applied to the input of this circuit. The tube acting with the grid resistor clipped and leveled the input wave thus giving a square current wave in the plate circuit. The

voltages developed by the higher harmonics of the current wave were emphasized by the inductive plate load. The harmonic-rich output of this signal was then applied to one of the grids of the 6A8 and there mixed with a signal from the local oscillator of the receiver. A 6A8 tube was used at this point rather than a 6L7 because the former was in stock and the latter was not. Audible beat frequencies between the harmonics of the input and the local oscillator signal were amplified in the next stage and applied to an oscillograph element.

Figure 13b is a typical record from this calibration circuit. The first two traces are the same as before and the last is the output from the 6J5. It can be seen that this trace periodically shows the envelope of the audio frequencies produced. Starting with the high frequencies, the amplitude of the envelope increased as frequency decreased until the low frequencies were reached where it began to decrease again and pass through zero at zero beat. The cycle was repeated as the frequencies were repeated on the other side. This trace gives a very clear indication of the precise location where zero beat occurred and permits the accurate determination of frequency for that point.

A 200-kilocycle signal was applied to the calibrating circuit input for the record of Fig. 13b. The eleventh

harmonic of this signal (2200 kilocycles) is responsible for the zero beat at the left end of the record. The local-oscillator frequency at this time was also 2200 kilocycles and since the intermediate-frequency amplifier was tuned at 465 kilocycles the receiver tuning at this time was 1735 kilocycles. The next major zero beats in order are with the twelfth harmonic at 1935 kilocycles, the thirteenth harmonic at 2135 kilocycles, and the fourteenth at 2335 kilocycles. Small zero beats can be seen between the major beats. They result from the second harmonic of the receiver's local oscillator. The first one occurs at 1835 kilocycles corresponding to a local-oscillator frequency of 2300 kilocycles. The second harmonic of this, namely 4600 kilocycles, beat with the twenty-third harmonic of the signal input to produce the record shown. Other beats of this kind occur at 2035 kilocycles and 2235 kilocycles.

On the first trace of the figure, it will be noted that signals were picked up at 1.8, 2.0 and 2.2 megacycles. Since nothing was being applied to the receiver while this record was being made, these traces show that there was leakage of the ninth, tenth, and eleventh harmonics from the calibrating circuit into the receiver. It is not surprising that leakage of this sort occurred

because the input voltage to the calibrator was high (10 volts) and the shielding between the circuits was not the best possible. This difficulty was not corrected because the circuit was abandoned for the reason indicated below.

Figure 13c is the calibration trace for a record similar to Fig. 13b but taken at a different time. While the first and last calibration pips on both records are coincident, the intermediate ones are far from being coincident. The discrepancy resulted from the existence of considerable slippage on the condenser drive shaft and belt slippage on the continuous-drive film holder. The position where this slippage occurred was uncertain and erratic; hence, it was impossible to identify frequencies which might appear on the record somewhere in between the calibration points. It was not easy to correct this difficulty and so the continuous-drive film holder was abandoned in favor of the magazine holder.

The film magazine holder consists of a drum around which a strip of record paper approximately 11 inches long can be drawn. If a definite relationship could be maintained between the position of the drum and the condenser shaft, the calibration of the records would be easy and since it would be the same on every record, comparisons between them would be greatly facilitated.

A direct connection between the shafts could have been made but the condenser rotation was only 180 degrees and this would use just one-half of the potential record length. Gears of the proper ratio were not available and so the drive shown in Fig. 12 was developed.

A semi-circular pulley was constructed and attached directly to the condenser shaft of the receiver. The diameter of this pulley was made slightly less than twice the diameter of the one on the film holder. A stout cord was permanently attached to one end of the condenser pulley, passed around it and on to the film holder pulley where again it was permanently attached. Neglecting a possible minor stretching of the cord, slightly under 360 degrees of rotation by the film holder gave a 180-degree rotation to the condenser. For each position of the film drum, there was a corresponding and fixed position of the condenser shaft.

A motor drive was provided to insure a relatively constant speed of rotation for the film drum. In a manner similar to the above, a cord was permanently attached to another of the film holder pulleys, passed around it and down to the slow speed shaft of a motor with a worm reduction where again it was permanently attached. Both the drive cords mentioned above and the driving motor can be seen clearly in Fig. 12.

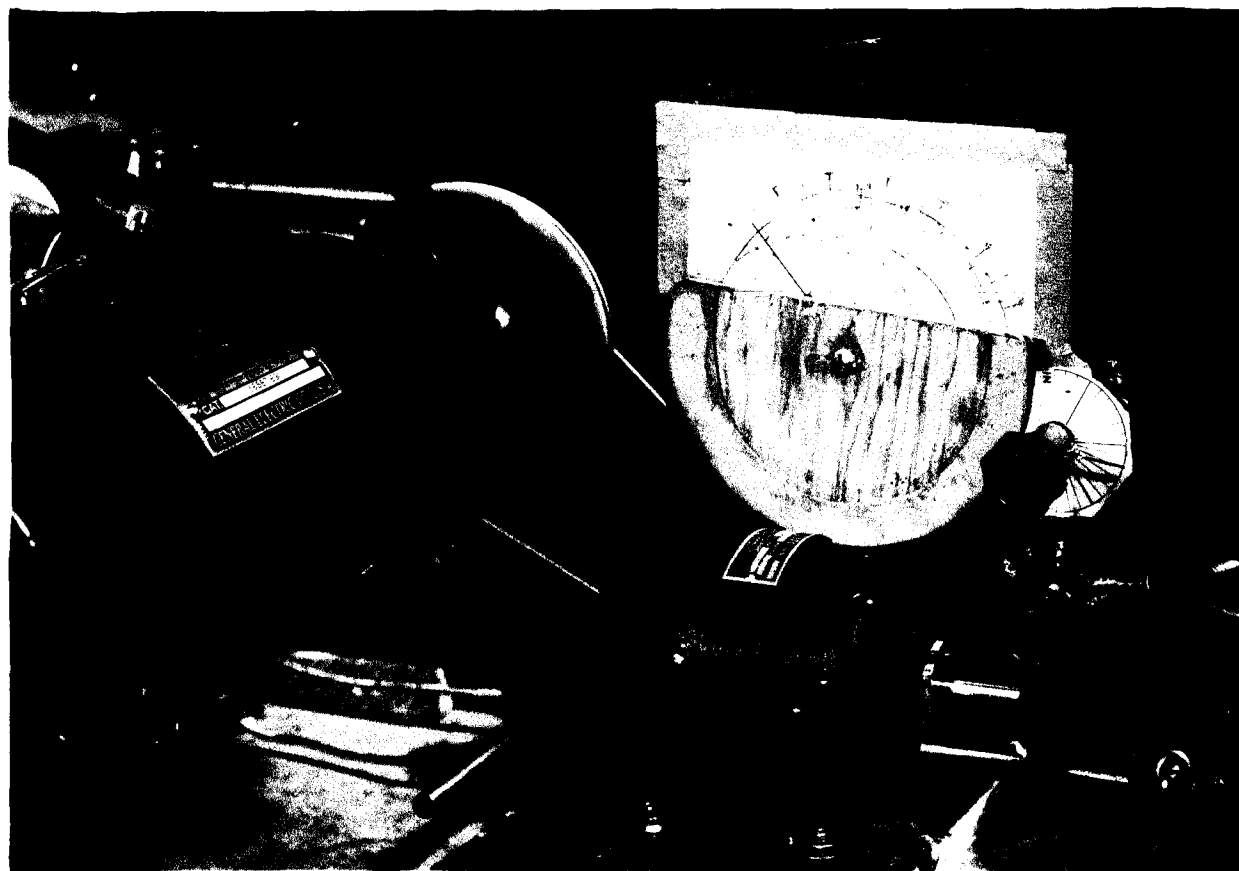


Fig. 12. Drive mechanism.

The curves which appear under the pointer on the condenser shaft were drawn to indicate the proper setting for the trimmer. As the tuning condenser was rotated by the motor, the trimmer was adjusted to the value indicated by these curves.

The rectifier used to supply power to the discharge tube was one which had been built for another project. The circuit diagram is given in Fig. 7. It consisted of a 15,000-volt center-tapped neon sign transformer feeding a pair of 878 rectifier tubes and filtered by a 1-microfarad 10,000-volt pyranol condenser. Due to a breakdown of the insulation on one of the filament transformers, however, it was necessary to run most of the test with the power supply operating as a half-wave rectifier. This was not a serious limitation because the current taken by the discharge tube was usually so small that the ripple from the supply was practically zero.

For awhile the magnitude of the current taken by the discharge tube was recorded along with the radio-frequency output. This was done by supplying the grid bias of a 6AG7 from a tap on the dropping resistor between the power supply and the discharge tube. An oscillograph element was connected between the plate and screen grid, and 90 volts were applied to the latter. The circuit was adjusted so

that the trace was along the bottom edge of the record paper when the bias was zero. The bottom trace in Fig. 13d is from this element. The center trace in the figure is the zero current position for both elements. Since the discharge current was found to have a negligible amount of variation in the time required to make a record, this circuit was only used for a portion of the runs on hydrogen.

III. RESULTS

A. Hydrogen

The negative point-to-plane corona of hydrogen was characterized by its relatively heavy current. This was to be expected, however, because of the very high mobility of the hydrogen molecules. Figure 14 shows the voltage and current relationships and indicates at a glance the range over which the observations were made. The general shape of these curves is as expected. At the lower pressures, the slope is greater and the current is higher. Some idea of the extent of the erratic performance of the point can also be obtained from these curves. For example, the curve for a pressure of 270 millimeters of mercury is almost coincident with that for 345 millimeters of mercury. Sometimes the current was even observed to increase or decrease spontaneously with no change in the applied voltage.

In nearly every case, a search through the bands of the receiver failed to reveal the presence of any radio-frequency radiation. There was just one exception. Some pick-up was obtained on the two lowest frequency bands when the pressure was 155 millimeters of mercury. Figure 13d

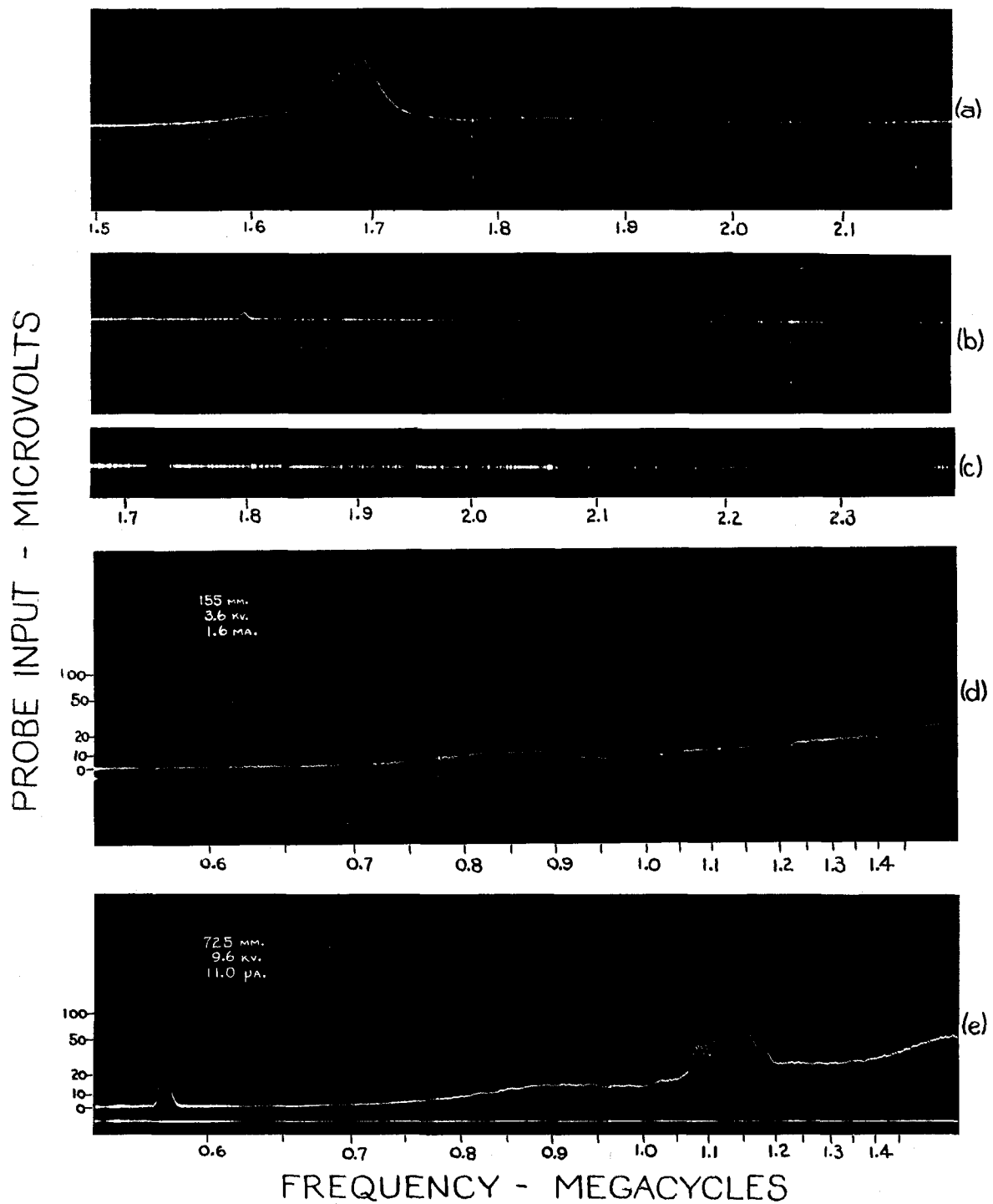


Fig. 13. (a), (b) and (c) Frequency calibration traces. (d) Spectrogram of hydrogen and simultaneous tube current. (e) Spectrogram of oxygen.

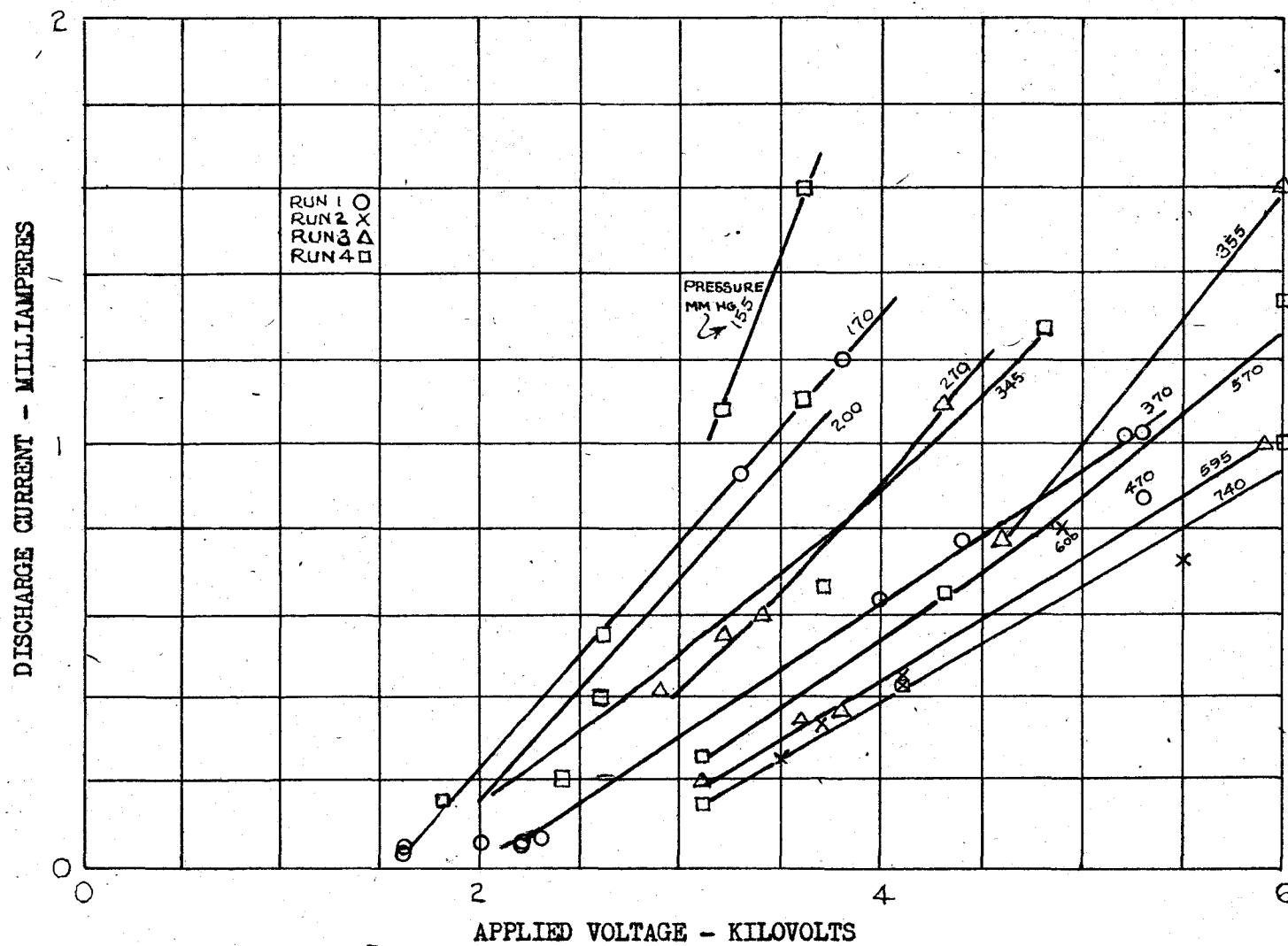


Fig. 14. Relationship between current and voltage for test runs on Hydrogen.

TABLE 3
Relationship Between Current and Voltage
For Test Runs on Hydrogen

Pressure mm Hg	Voltage Kilo- volts	Current Milli- amperes	Pressure mm Hg	Voltage Kilo- volts	Current Milli- amperes
(Run 1)					
470	5.3	0.88	740	5.5	0.73
370	5.3	1.03	740	4.1	0.46
370	5.2	1.02	740	4.1	0.44
370	4.4	0.78	740	3.7	0.34
370	4.0	0.65	740	3.5	0.24
370	2.3	0.08	600	4.9	0.80
370	2.2	0.07			
370	2.2	0.06			
370	2.0	0.07			
170	3.8	1.20			
170	3.3	0.93			
170	1.6	0.05			
170	1.6	0.03			
(Run 3)					
595	5.9	1.00	740	6.0	1.00
595	3.8	0.38	740	4.1	0.44
595	3.6	0.36	740	3.1	0.16
595	3.1	0.20	570	6.0	1.34
355	6.0	1.60	570	4.3	0.66
355	4.6	0.77	570	3.1	0.26
270	4.3	1.10	345	4.8	1.28
270	3.4	0.60	345	3.7	0.68
270	3.2	0.56	345	2.6	0.56
270	2.9	0.41	345	2.4	0.20
			200	3.6	1.10
			200	2.6	0.40
			200	1.8	0.15
			155	3.6	1.60
			155	3.2	1.08
(Run 4)					

is the spectrogram of one of these bands. A spectrogram was also made of the other band, but it showed no radiation at all. In other words, the radiation had spontaneously disappeared in the short time required to reel in a new strip of record paper and start the run. It had also disappeared from the other band.

The cathode-ray picture of current showed a high-frequency square wave superimposed on the ripple. It did not change with the disappearance of the radio-frequency energy. Usually the cathode-ray picture for other runs simply showed the characteristic sawtooth form of the ripple with nothing superimposed, but there were a good many runs with either superimposed pips or fine grass. Radio-frequency output was not observed on any of them. In all cases, the ripple was quite pronounced because the current taken by hydrogen was always excessively large for the power supply used.

Just prior to the above observation, a run had been made at a pressure of 145 millimeters of mercury. At this pressure a sort of moderately slow relaxation oscillation was set up. The condenser of the power supply periodically discharged through the tube with a high current. During the discharge period, the surface of the electrode was covered with cathode glow for a distance

of about one-quarter inch from the end. Since the performance in this region was so unstable, the pressure was increased for the next observation. Apparently the point was temporarily modified by the above operation in such a way as to make generation of radio frequencies possible.

The probe-input scale on the left of the spectrogram only applies at the middle frequency range of the record. In order to determine the approximate output at other frequencies, the variation of receiver sensitivity with frequency must be taken into account. Figure 16a indicates the nature of this variation for the low-frequency band. The strips shown were cut from a long continuous-drive spectrogram. Consequently, the width of the resonance peaks are close to double what they would be on one of the magazine spectrograms. Each resonance peak was made with a 50-microvolt input to the probe.

A tracing was made of a line passing through the peaks of the resonance curves. When this tracing was placed over Fig. 13d, it was found that the spectrogram trace followed the trend of the receiver sensitivity quite closely showing that the magnitude of the radio-frequency output was fairly uniform over the band. The spectrogram shows that the input to the probe was approximately 10 microvolts.

It will be noted that the spectrogram of Fig. 13d is wider than any of the rest. The others have all been trimmed to permit better arrangement on the page. This one was not trimmed so that it could be used to illustrate the general appearance of the original records.

B. Oxygen

In contrast with hydrogen, radio-frequency output was observed on all runs with oxygen except those at very low pressures (8 millimeters of mercury). All of the points at which spectrograms of radiation were made have been plotted on the voltage-current characteristics of Fig. 15. The same general trends and erratic performance which were noted on Fig. 14 are also present here. The major difference between the two figures is that the magnitudes of currents taken by oxygen were considerably lower and the applied voltages were somewhat higher.

The last three spectrograms of Fig. 16 show the characteristic continuous-band radio-frequency spectrum of oxygen near atmospheric pressure. Using a tracing of the receiver sensitivity characteristic as explained above, it can be shown that Fig. 16c represents a practically uniform, continuous-band, 50-microvolt input to the probe. On

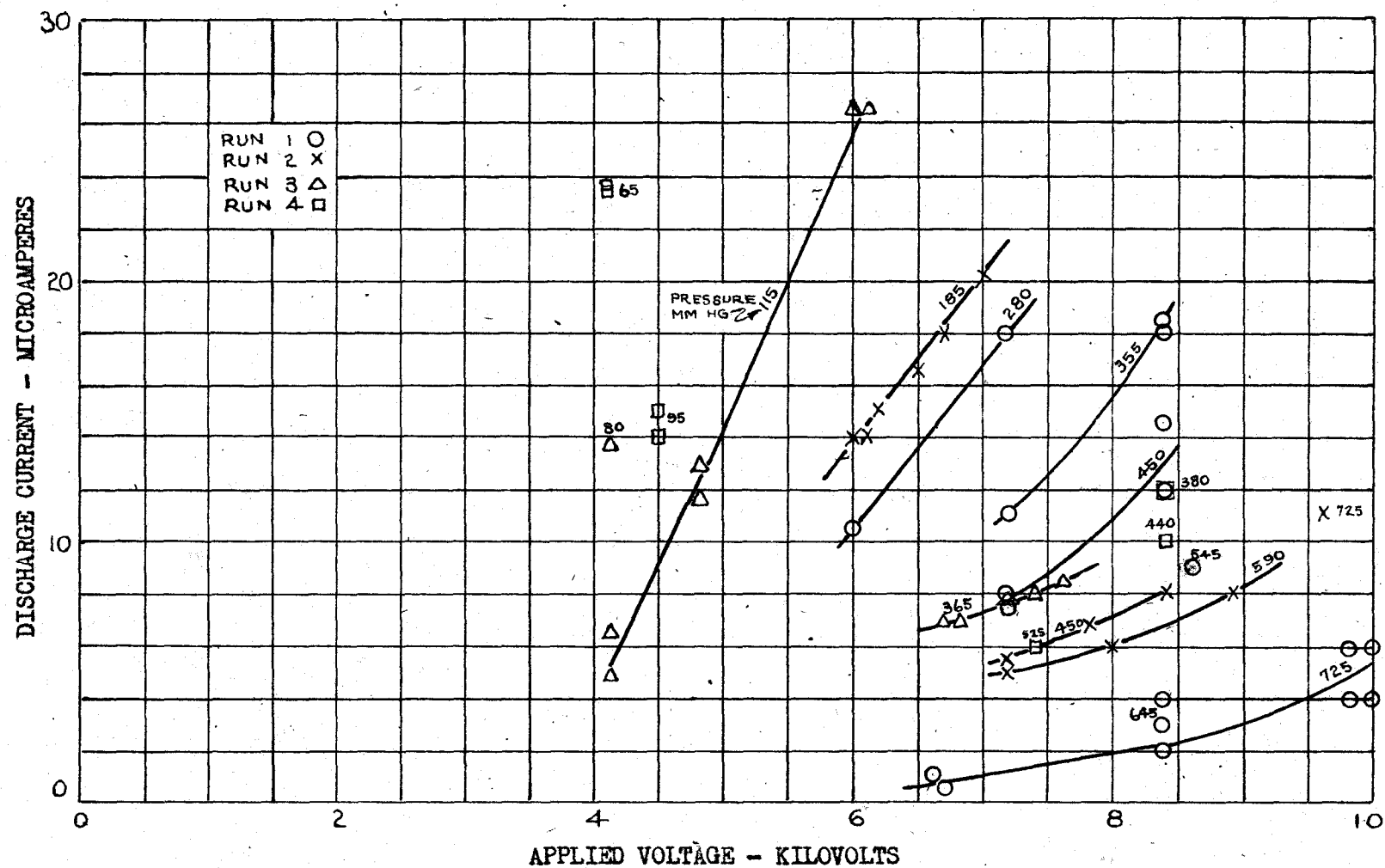


Fig. 15. Relationship between current and voltage for test runs on Oxygen.

TABLE 4

Relationship Between Current and Voltage
For Test Runs on Oxygen

Pressure mm Hg	Voltage Kilo- volts	Current Milli- amperes	Pressure mm Hg	Voltage Kilo- volts	Current Milli- amperes
(Run 1)			(Run 2)		
725	10.0	4-6	725	9.6	11.0
725	9.3	4-6	590	8.9	8.0
725	8.4	2.0	590	8.0	6.0
725	6.7	0.4	590	7.2	5.0
725	6.6	0-1	450	8.4	8.0
645	8.4	3-4	450	7.8	6.6
545	8.6	9.0	450	7.2	5.4
450	8.4	14.4	450	7.2	5.0
450	8.4	12.0	185	7.0	20.2
450	7.2	8.0	185	6.7	18.0
450	7.2	7.4	185	6.5	16.4
355	8.4	18.0	185	6.2	15.0
355	8.4	17.4	185	6.1	14.0
355	7.2	11.0	185	6.0	14.0
280	7.2	18.0			
280	6.0	10.4			
(Run 3)			(Run 4)		
365	7.6	8.4	525	7.4	6.0
365	7.4	8.0	440	8.4	10.0
365	7.2	7.8	380	8.4	12.0
365	6.8	7.0	95	4.5	15.0
365	6.7	7.0	95	4.5	14.0
115	6.1	26.4	65	4.1	23.2
115	6.0	26.4	65	4.1	22.6
115	4.8	13.0			
115	4.8	11.6			
115	4.1	6.4			
115	4.1	4.8			
80	4.1	13.8			

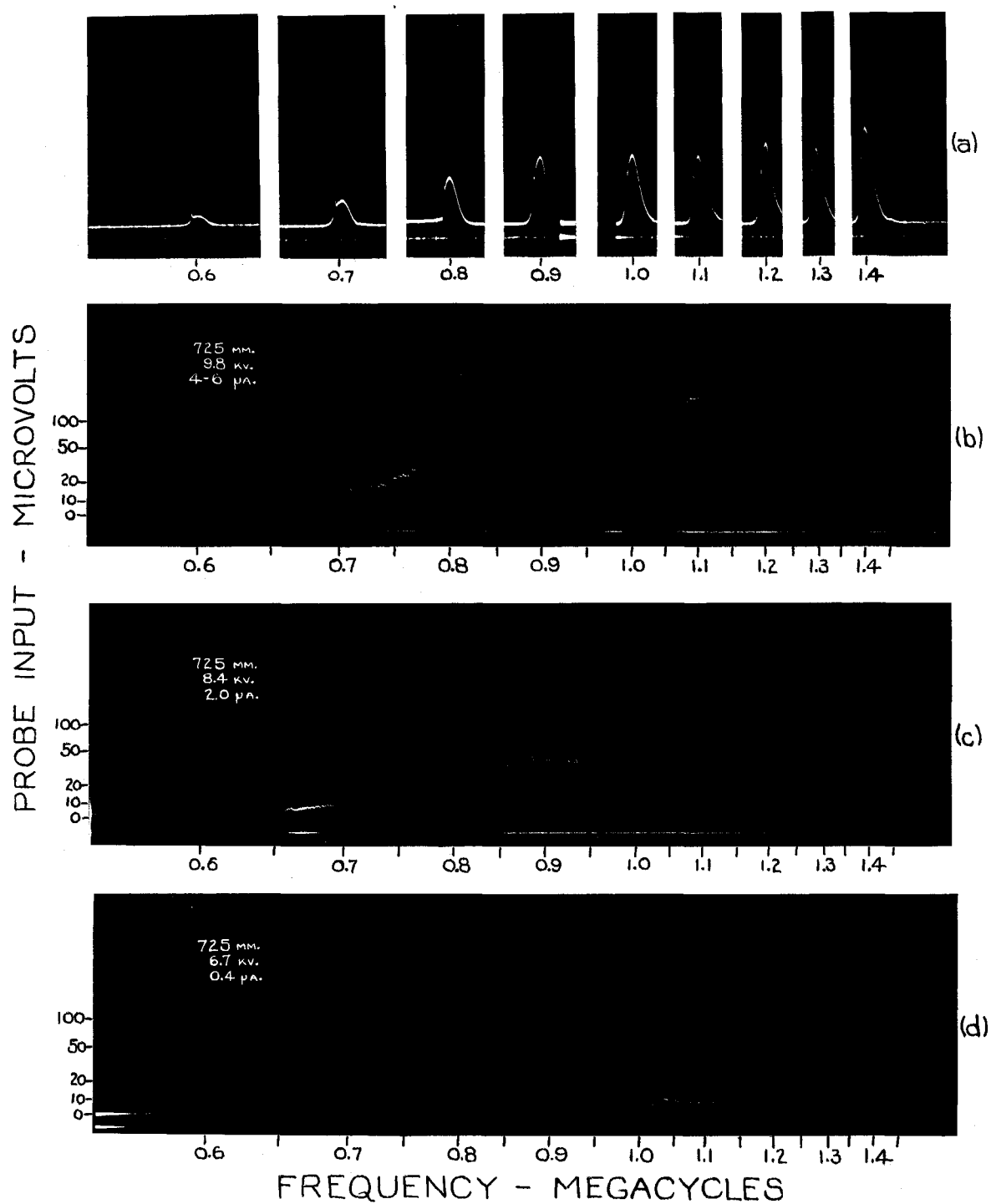


Fig. 16. (a) Receiver outputs for 50-microvolt probe inputs. (b), (c) and (d) Spectrograms for oxygen near atmospheric pressure.

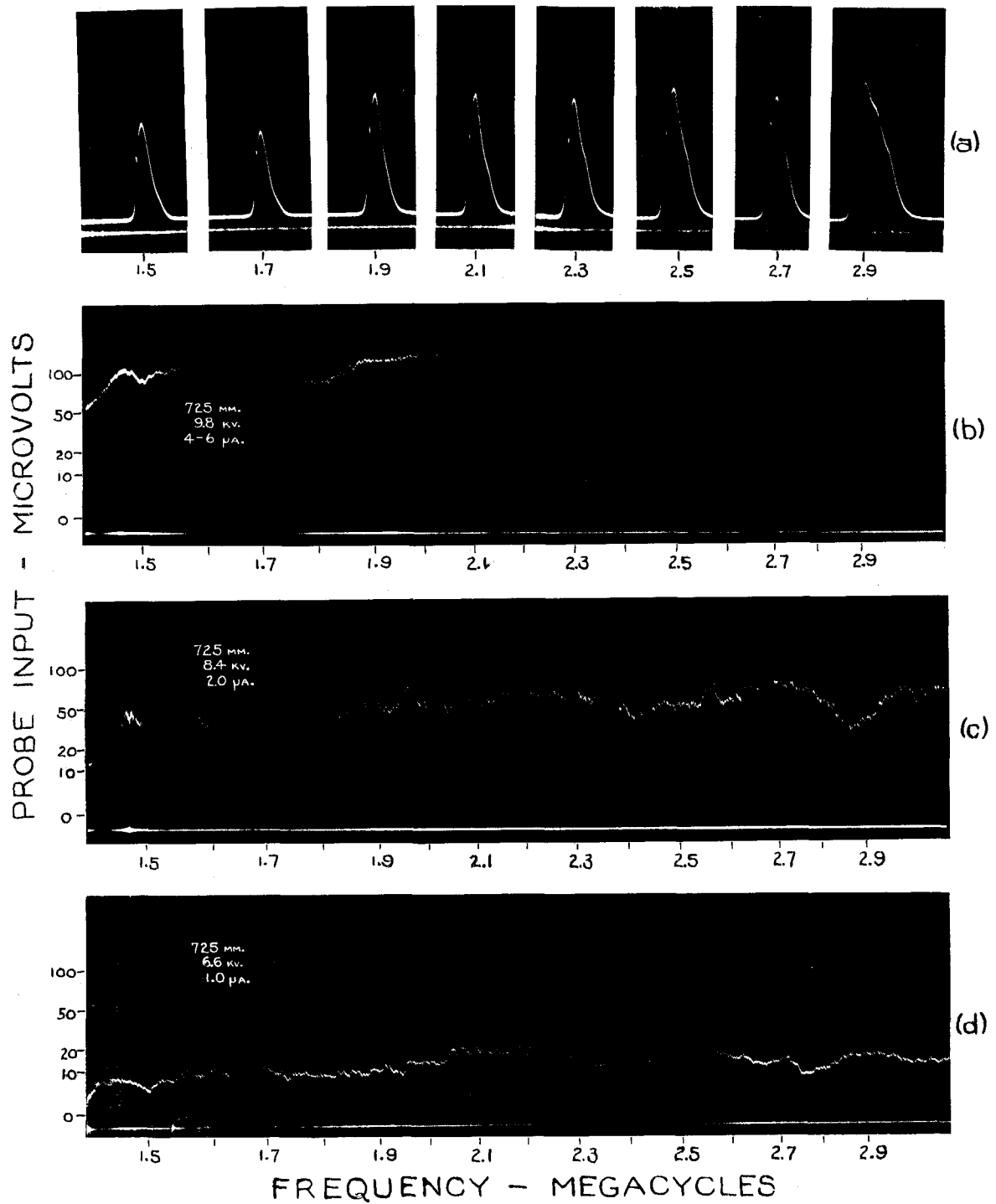


Fig. 17. (a) Receiver outputs for 50-microvolt probe inputs. (b), (c) and (d) Spectrograms for oxygen near atmospheric pressure.

the other hand, Fig. 16b shows a somewhat greater output on the high-frequency end than it shows near the middle. The probe input near the middle is about 80 microvolts. Figure 16d shows a practically uniform input to the probe of about 3 microvolts.

From the spectrograms of Fig. 16, it can be said that the radio-frequency output from a negative-point discharge in oxygen is practically uniform over the frequency range 0.55 to 1.6 megacycles. The intensity of the oscillation is an increasing function of the applied voltage.

Figure 17 gives a set of spectrograms for the frequency range 1.4 to 3.0 megacycles which parallels those of Fig. 16. Again the spectrum is continuous and practically uniform over the band. As before, the input to the probe was about 80 microvolts when the voltage applied to the tube was 8.4 kilovolts. At the higher and lower voltages, however, the output in this band was somewhat greater than it was in the lower frequency band. The input to the probe was over 100 microvolts when the tube voltage was 9.8 kilovolts, and it was about 20 microvolts when the tube voltage was 6.6 kilovolts. Again the intensity of oscillations is an increasing function of the voltage.

Similar spectrograms were also made for the other frequency ranges of the receiver. The same general trends were observed, but the intensity of the oscillations fell off considerably as the higher frequencies were approached. These and subsequent observations indicated that most of the radiation was occurring in the two lower frequency bands of the receiver; therefore, observations were confined almost exclusively to them.

The cathode-ray oscillograph picture of current for these runs showed a series of pulses like those described by Trichel. As the voltage was increased, these pulses occurred closer and closer together until the picture on the oscillograph had the appearance of dense grass.

Occasionally strong narrow bands of frequencies were found superimposed on the continuous spectrum. An example of such a spectrogram is given in Fig. 13e. This record was made on a different day than the ones discussed above. The current input was relatively greater and the radio-frequency output relatively less than on them. The cathode-ray picture showed only few pips along the trace. These indicated that current dropped to zero momentarily and then returned to its steady value. This was in contrast with the dense grass which had been observed before. Between the two runs, the tube had been pumped to a high

vacuum and refilled with oxygen. It is possible that there were dust specks on the cathode during the earlier run and that they were loosened by some of the discharges at low pressure and removed during the evacuation process.

Figures 18a and 18b are two spectrograms which were made a few minutes apart under identical conditions. Figure 18d is a double trace spectrogram which was taken at the same time to illustrate the same point. Figure 18c is a typical single trace spectrogram which was made at a tube voltage between the other two. These records clearly show that the character of the spectrum can change quite radically from one moment to the next. This observation led to the adoption of the multiple-trace technique in making all subsequent records.

The above spectrograms were actually taken at increasing increments of voltage and so the time order is the reverse of the order on the page. The fairly steady signal appearing around 2.6 megacycles in Fig. 18d gradually decreased in frequency to 2.4 megacycles. On the other hand, the signal starting at 1.7 megacycles increased in frequency at first. Then it decreased, broadened and disappeared. Of course, there is no positive assurance that each of the disturbances traced above are really gradual transitions of the same signal. It is

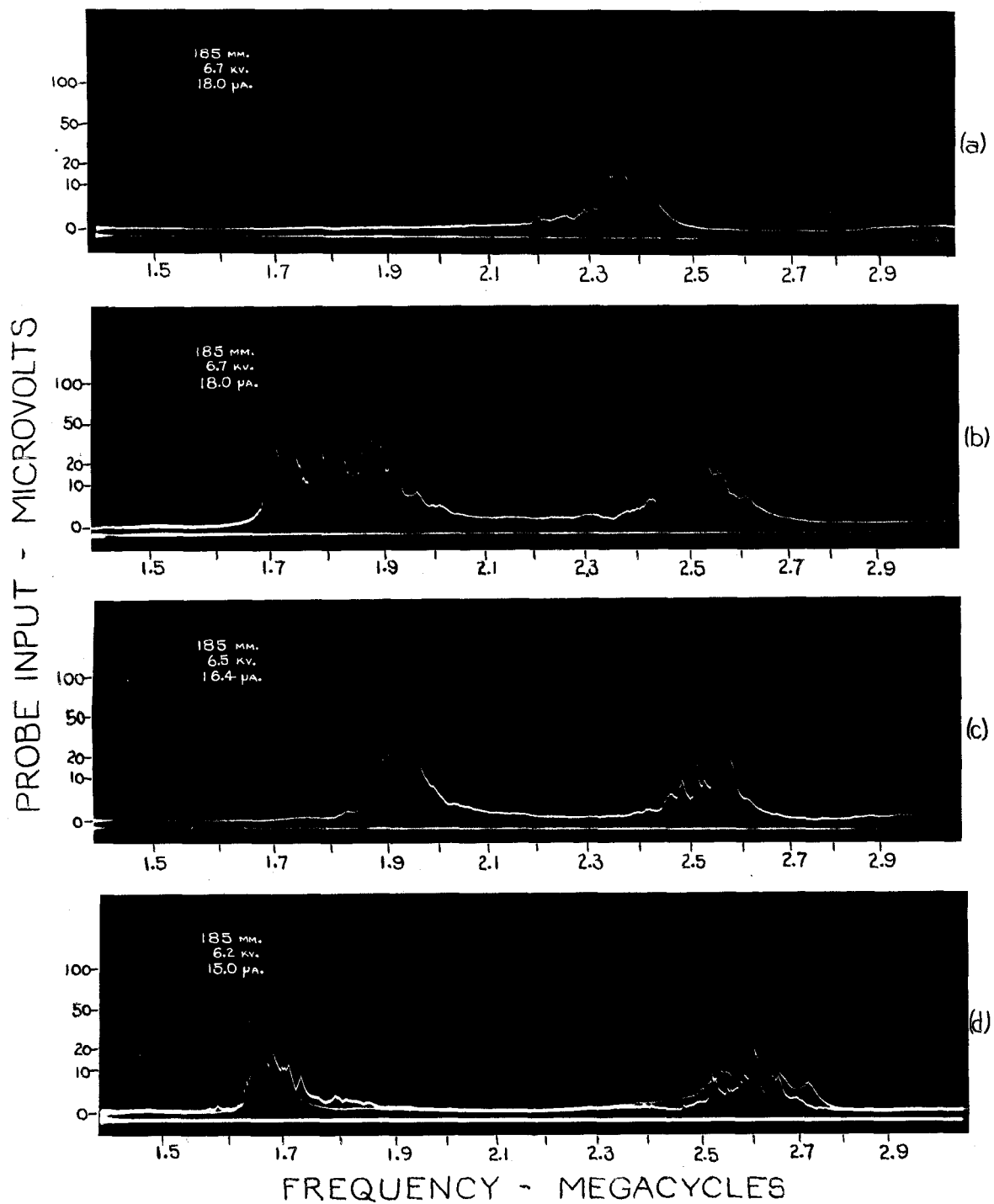


Fig. 18. Early spectrograms for oxygen at low pressure.

entirely possible that they represent separate disturbances which arose and then disappeared.

Figures 19 and 20 were made by the multiple-trace technique to illustrate the effect of changing the applied voltage. They are arranged on both pages in the order they were taken except Figs. 20c and 20d which were erroneously interchanged during the mounting process. The spectrograms in Fig. 19 tend to indicate that a particular voltage leads to stabilized oscillation about fixed frequencies. However, the voltage (7.4 kilovolts) which gives the most stable oscillation in the spectrograms of Fig. 20 is different from that of Fig. 19 (7.6 kilovolts).

As before, a signal appearing for the first time at 0.97 megacycles in Fig. 19b seems to have gradually shifted to 0.95 megacycles. At the same time, a signal appearing at 1.45 megacycles in Fig. 19a seems to have shifted back and forth between 1.35 and 1.47 megacycles.

Similar trends together with the apparently spontaneous appearance and disappearance of frequencies can also be traced in Fig. 20. The cathode-ray picture of the current for the runs discussed above indicated that there were no alternating-current components.

Spectrograms made at higher pressures show the same general trends. The major difference between their

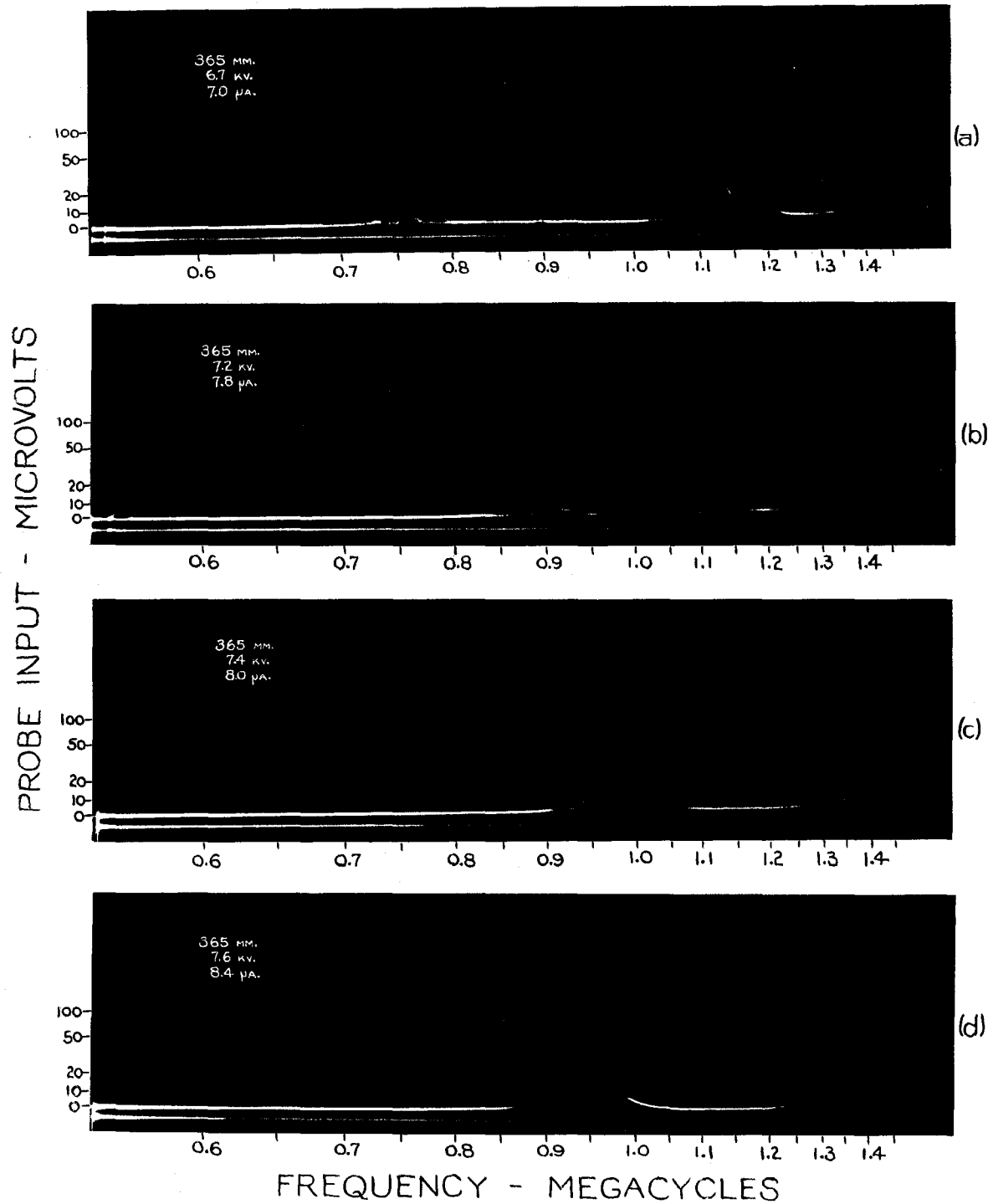


Fig. 19. Spectrograms for oxygen at medium pressure illustrating the effect of different applied voltages.

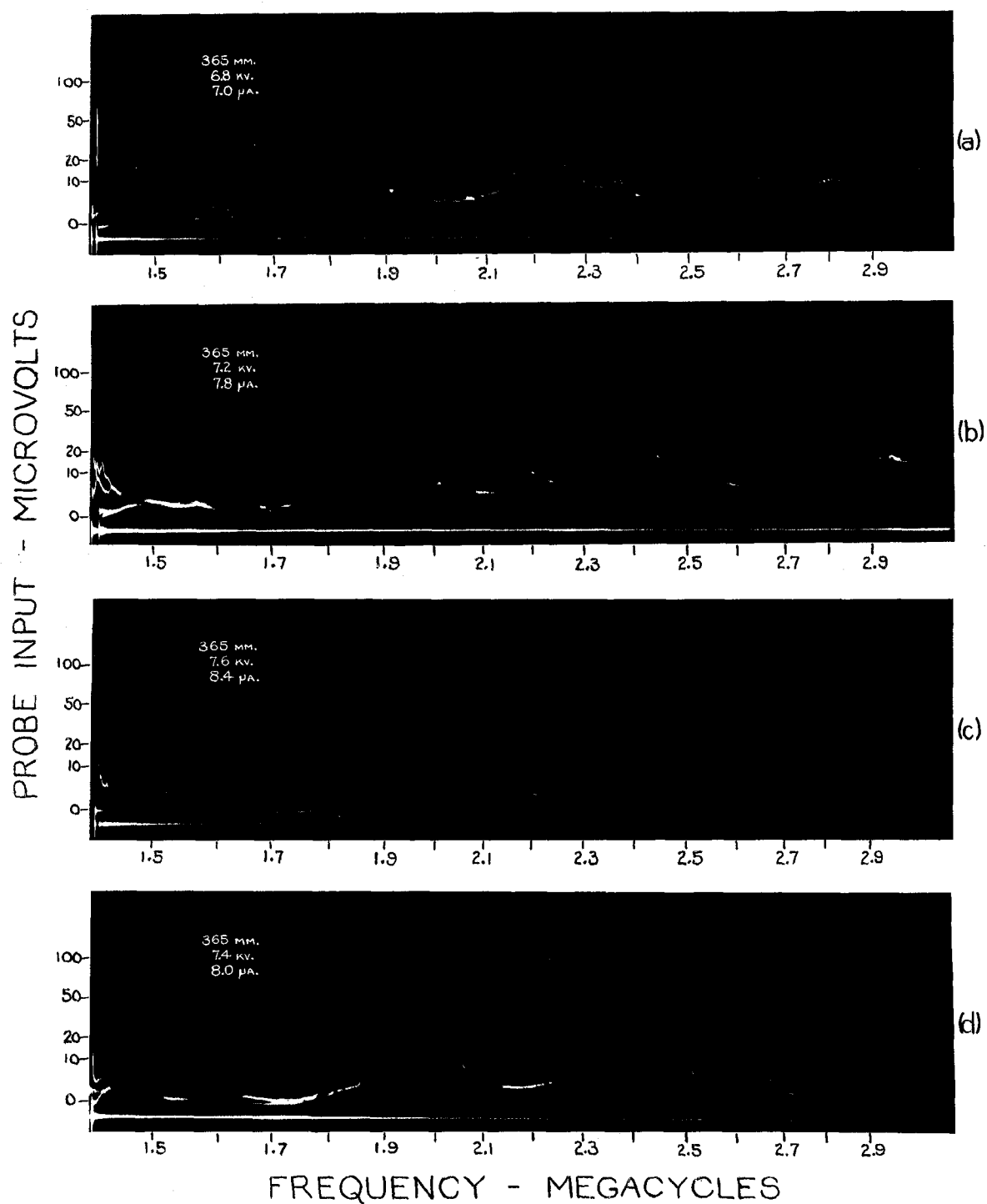


Fig. 20. Spectrograms for oxygen at medium pressure illustrating the effect of different applied voltages.

appearance and the appearance of the spectrograms presented in the figures is that the peaks of energy are somewhat broader and sometimes merge into a continuous band.

On the other hand, Figs. 21 and 22 show the appearance of typical low-pressure spectrograms. The energy in these cases is confined to rather narrow bands. It is almost of a single frequency nature.

Figure 21c is a spectrogram of some of the most highly stabilized oscillations which were produced. It can be seen that two of the frequencies appearing in this figure also seem to occur in Figs. 21a and 21b. All of these were taken under greatly different conditions, and so the effect is probably coincidental rather than of real significance.

When the voltage applied to the discharge tube was too high, the oscillations disappeared. This effect is shown in Fig. 21d. It was taken at a voltage near the transition point and shows that the radio-frequency oscillations occurred during only one of the traces. It should be compared with Fig. 22a which was taken under the same circumstances but at a lower voltage.

Figures 22b and 22c were made under identical conditions a few minutes apart. They clearly illustrate that even multiple-trace spectrograms can only be considered as

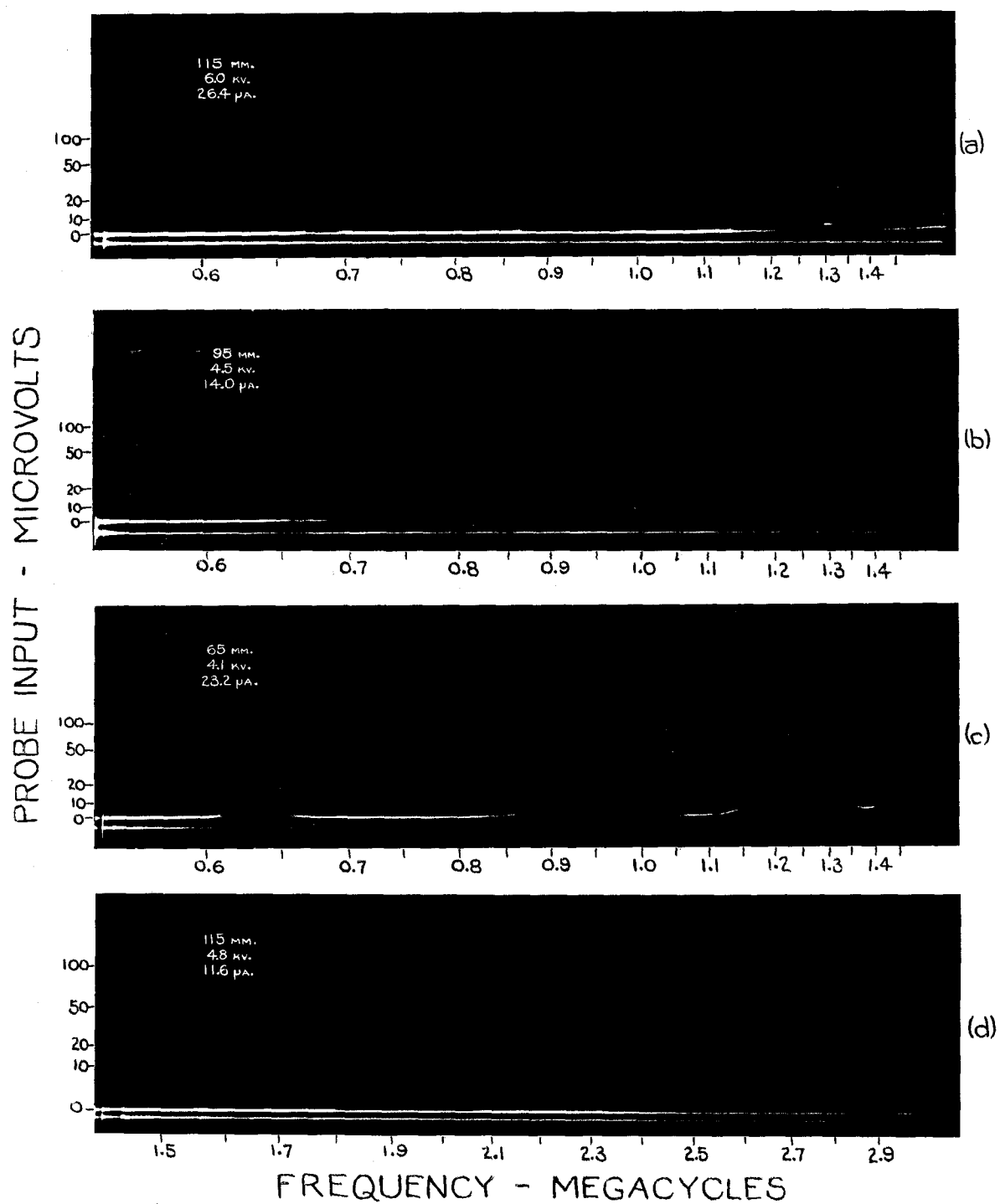


Fig. 21. Spectrograms for oxygen at low pressures.

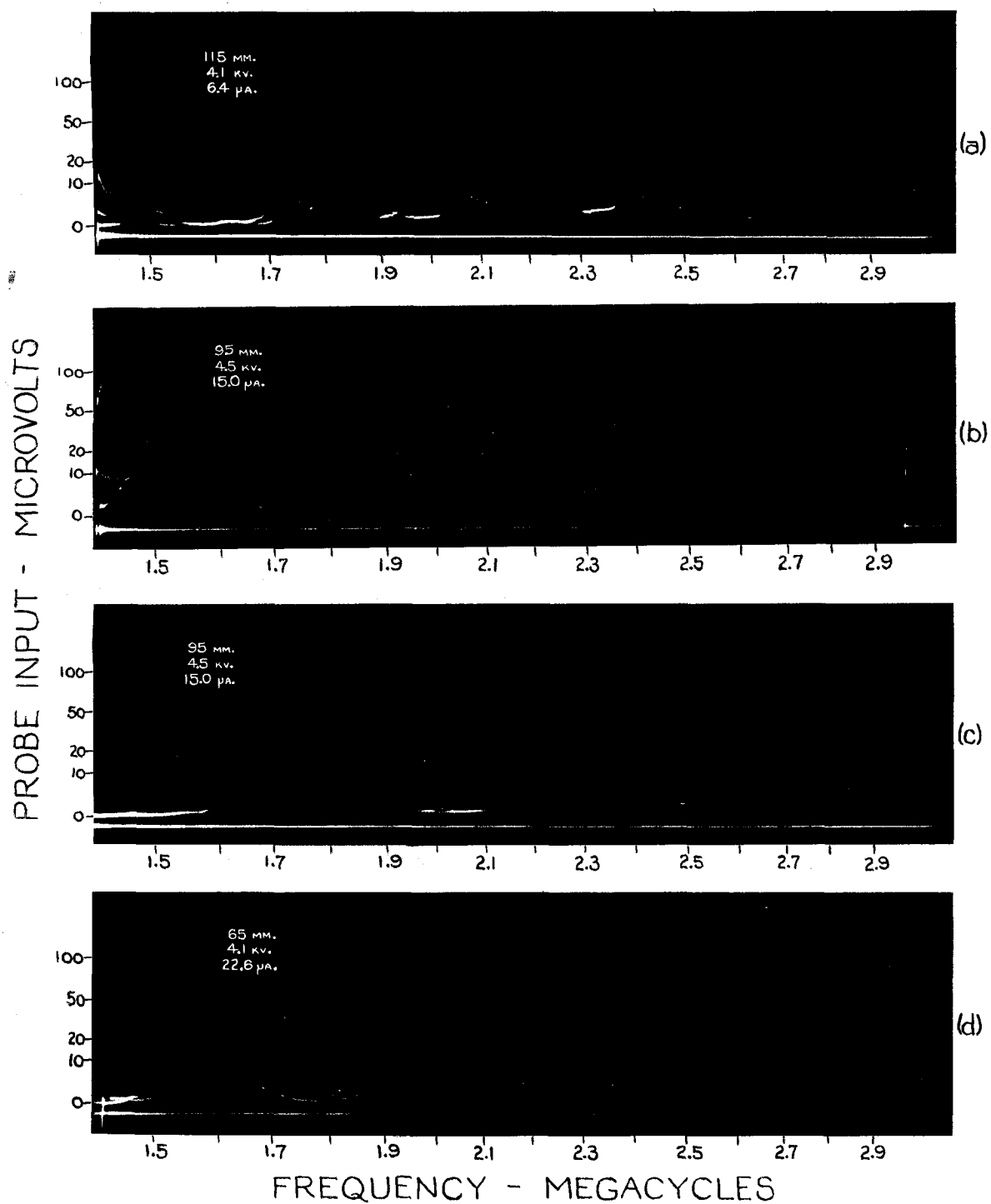


Fig. 22. Spectrograms for oxygen at low pressures.

records of the radio-frequency spectrum during the interval of time that the observation was being made.

The cathode-ray picture of the current for all the runs in Figs. 21 and 22 showed no alternating-current components.

IV. DISCUSSION

The most significant observation was that oxygen always gave a radio-frequency output and hydrogen never did except for a very brief period. The fact that there was radiation which disappeared after a few minutes indicates that the element responsible for the output was removed in some manner. At the same time, it is well to recall that an extensive cathode glow discharge at low pressure was apparently responsible for initiating the conditions which led to the production of radiation.

Corona discharge in hydrogen converts it to a very active form which readily reduces oxides. For this reason, there can be little doubt that the tungsten point had a clean metallic surface in the vicinity where the corona was formed. Temporary exposure to the extensive glow discharge may have started reduction of the oxide on the point through fissures near the end. Increasing the pressure slightly would narrow the area over which the discharge originated but still keep it large enough to include some of the newly opened fissures. As the discharge progressed, more and more of the oxide surrounding the fissure would be reduced until a relatively large bare metallic surface was produced.

With oxygen in the tube, it is practically certain that there was never very much surface area on the point which was not covered with oxide. This is assured by the fact that ozone is generated during the discharge. The oxide coating had to be continually broken down to allow passage of the arc current. In a short time, the fissures developed would tend to be sealed by the oxidation process.

The existence of small fissures through which a portion of the arc current could flow would cause periodic interruption of that portion by a process like that described by Kleinwachter. Of course, the apertures used in his work were very much larger than the size of apertures which are being supposed here, but the pressures involved are also very much lower.

The above theory for the origin of the radio-frequency radiation from a point-to-plane discharge permits a logical explanation for all the phenomena observed. The portion of current involved in a particular oscillation would probably be so small that it would not be noticed on the cathode-ray oscillograph trace; hence, there need not be a correlation between the gross appearance of this trace and the frequencies produced. The tendency for the frequency of a particular signal to either increase or decrease with time could be explained on the basis that a fissure is either

being closed by further oxidation or being opened by breakdown of the oxide. Other theories do not allow erratic performance of this sort. The fact that very few of the oscillations occurring at a given time bear harmonic relationships indicates that they have separate origins. The more erratic character of the oscillations at the higher pressures could be due to the fact that more gas molecules are present; hence, the building up and tearing down processes would take place at a more rapid rate. The continuous band observed at atmospheric pressure could easily arise from rapid shifts of the generated frequencies.

The proposed theory is substantiated by the observation that the tungsten point was always cleaned of oxide near the tip after a series of discharges in hydrogen and was always covered with oxide after a series of discharges in oxygen. Nevertheless, it remains pure conjecture because some important points cannot be checked with the present apparatus. Foremost among these is the question of just how the frequency shift takes place from one moment to the next. A broad-band panoramic receiver would be required for such an observation. A receiver of this sort would also assist in checking another important point.

The pressure could be shifted slightly while under observation to see if a frequency shift were made in the proper direction.

Some observations should be made on gases which would not react with either the oxide or the metal. They could be tested on clean electrodes and then on oxide-covered electrodes to see if whether or not the performance were different in the two cases.

V. SUMMARY

Radiation in the range from 0.55 to 3.0 megacycles arising from a negative point-to-plane corona discharge in a pure hydrogen and pure oxygen has been studied over a wide range of pressures. A recording receiver was used to make radio-frequency spectrograms of the output produced.

In general, no radiation was obtained from the discharge in hydrogen. Radiation which was produced under an exceptional circumstance disappeared after the discharge had been running for a short length of time. It was attributed to the presence of an oxide film on the cathode which was reduced by continued exposure to the activated hydrogen.

Radiation was obtained from all discharges in oxygen except those at very low pressure. A continuous-band spectrum was produced at the pressures near atmospheric. It broke up into narrow bands and finally into single frequency signals as the pressure was reduced. Usually the frequency of the radiated signals did not remain fixed. Instead it appeared to gradually wander over the entire band.

A tentative explanation of the process is made on the basis that the oscillations probably arise from the periodic extinction of arcs passing through fine fissures in the oxide layer covering the cathode.

VI. REFERENCES

1. Adirovich, E. Oscillations and relaxation processes in the electron plasma of the discharge. Comptes Rendus Akademifa nauk SSSR (Doklady) 48:551-554. 1945.
2. _____ Propagation of waves and retardation of electron beams in plasma. Comptes Rendus Akademifa nauk SSSR (Doklady) 48:630-632. 1945.
3. Cobine, J. D. and Gallagher, C. J. Noise and oscillations in hot cathode arcs. Jour. Franklin Inst. 243:41-54. 1947.
4. Engelhardt, V. The electrolysis of water processes and applications. Easton, Pa., The Chemical Publishing Co. 1904.
5. Fox, G. W. Oscillations in the glow discharge in argon. Phys. Review ser. 2, 37:815-820. 1931.
6. Ginzton, E. L. D-C amplifier design techniques. Electronics 17, no. 3:98-102. March, 1944.
7. Granovsky, B. L. and Bykhovskaya, L. N. Characteristic electric oscillations of a low pressure mercury arc. Comptes Rendus Akademifa nauk SSSR (Doklady) 49:339-342. 1945.

8. Granovsky, B. L. and Suetin, T. A. The generation of high-power electric oscillations by a low pressure discharge. Comptes Rendus Akademika nauk SSSR (Doklady) 49:410-413. 1945.
9. Harnett, D. E. and Case, N. P. The design and testing of multirange receivers. Proc. I.R.E. 23:578-593. 1935.
10. Heldman, J. D. Techniques of glass manipulation in scientific research. New York, Prentice Hall, Inc. 1946.
11. Hudson, G. G. Negative point-to-plane corona in air. Phys. Review ser. 2, 61:205. 1942.
12. Kleinwächter, H. Schwingungserscheinungen bei stark eingegengter Lichtbogensäule und bei anomalen Anodenfall. Arch. f. Elek-tech. 34:523-530. 1940.
13. Klemperer, O. Prevention of capillary disturbances in electrolytic field plotting troughs and in McLeod gauges. Jour. Scien. Instr. 21:88. 1944.
14. Linder, E. G. Effect of electron pressure on plasma electron oscillations. Phys. Review ser. 2, 49:753-754. 1936.
15. _____ Attenuation of electromagnetic fields in pipes smaller than critical size. Proc. I.R.E. 30:554-556. 1942.

16. Loeb, L. B. Fundamental processes of electrical discharge in gases. New York, John Wiley & Sons, Inc. 1939.
17. Reiff, H. J. Ein neues Kompressions-Vakuummeter mit direkt ablesbarer linearer Teilung und mehreren dekadischen Messbereichen nebst einer Skizze der Entwicklung dieser Instrumententype. Zeits. f. Instrumentenkunde 34:97-106. 1914.
18. Rittner, E. S. A Pirani Gauge for use at pressures up to 15 mm. Review Solen. Instr. 17:113-114. 1946.
19. Rosenberg, P. A method for diminishing the sticking of mercury in capillaries. Review Solen. Instr. 9:258-259. 1938.
20. Seeliger, R. Zur Theorie der Elektronen-Plasmaschwingungen. Zeits. f. Physik 118:618-623. 1941/1942.
21. Smythe, W. R. and Michels, W. C. Advanced electrical measurements. pp. 179-184. New York, D. Van Nostrand Co., Inc. 1932.
22. Taylor, H. S. Industrial hydrogen. pp. 102-122. 171-200. New York, The Chemical Catalog Co., Inc. 1921.
23. Tonks, L. and Langmuir, I. Oscillations in ionized gases. Phys. Review ser. 2, 33:195-210. 1929.

24. Trichel, G. W. The mechanism of the negative point-to-plane corona near onset. Phys. Review ser. 2, 54:1078-1084. 1938.
25. Wright, R. H. Manual of laboratory glass-blowing. pp. 60-63. Brooklyn, Chemical Publishing Co., Inc. 1943.
26. Zeleny, J. Some observations on electrical discharges from pointed conductors. Jour. Franklin Inst. 232:23-37. 1941.

VII. ACKNOWLEDGMENT

Many members of the Iowa State College staff have been most helpful in lending assistance which materially aided in the completion of this work. Their cooperation is sincerely appreciated. In particular, the writer wishes to thank Dr. J. D. Ryder and Prof. W. L. Cassell for their suggestions, interest and encouragement.

VIII. VITA

Author: Willis Laurens Emery

Father's name: William Lorenzo Emery

Mother's name: Sarah Laurens Nebeker

Date and place of birth: November 23, 1915

Salt Lake City, Utah

Elementary and high schools attended:

Jackson School, Salt Lake City, Utah

West High School, Salt Lake City, Utah

Universities attended:

University of Utah, Salt Lake City, Utah

Iowa State College, Ames, Iowa

Degrees: Bachelor of Science, University of Utah, 1936

Master of Science, Iowa State College, 1940

Field of Specialization: Electrical engineering,

electronics and communications

Professor in charge of major work: Dr. J. D. Ryder

Doctoral committee: Dr. J. D. Ryder

Dr. W. B. Boast

Dr. L. T. Earls

Dr. J. J. L. Hinrichsen

Dr. G. Murphy